J Neurophysiol 101: 2632–2648, 2009.
First published February 18, 2009; doi:10.1152/jn.91213.2008.

Repetition Priming Influences Distinct Brain Systems: Evidence From Task-Evoked Data and Resting-State Correlations

Gagan S. Wig,[1,3] Randy L. Buckner,[1,2,3] and Daniel L. Schacter[1,3]

[1]*Department of Psychology and* [2]*Center for Brain Science and Howard Hughes Medical Institute, Harvard University, Cambridge; and* [3]*Athinoula A. Martinos Center for Biomedical Imaging, Massachusetts General Hospital, Charlestown, Massachusetts*

Submitted 11 November 2008; accepted in final form 17 February 2009

Wig GS, Buckner RL, Schacter DL. Repetition priming influences distinct brain systems: evidence from task-evoked data and resting-state correlations. *J Neurophysiol* 101: 2632–2648, 2009. First published February 18, 2009; doi:10.1152/jn.91213.2008. Behavioral dissociations suggest that a single experience can separately influence multiple processing components. Here we used a repetition priming functional magnetic resonance imaging paradigm that directly contrasted the effects of stimulus and decision changes to identify the underlying brain systems. Direct repetition of stimulus features caused marked reductions in posterior regions of the inferior temporal lobe that were insensitive to whether the decision was held constant or changed between study and test. By contrast, prefrontal cortex showed repetition effects that were sensitive to the exact stimulus-to-decision mapping. Analysis of resting-state functional connectivity revealed that the dissociated repetition effects are embedded within distinct brain systems. Regions that were sensitive to changes in the stimulus correlated with perceptual cortices, whereas the decision changes attenuated activity in regions correlated with middle-temporal regions and a frontoparietal control system. These results thus explain the long-known dissociation between perceptual and conceptual components of priming by revealing how a single experience can separately influence distinct, concurrently active brain systems.

INTRODUCTION

Repetition facilitates the ability to recognize and classify stimuli in our environment—a process that allows us to navigate our surroundings with greater ease and fluency. The performance enhancement that accompanies repetition is referred to as "behavioral priming," a type of implicit memory that can occur outside the realm of conscious awareness (Roediger and McDermott 1993; Schacter 1987; Tulving and Schacter 1990) and is typically preserved in amnesic patients (Cave and Squire 1992; Graf and Schacter 1985; Warrington and Weiskrantz 1974) and older adults (e.g., Fleischman and Gabrieli 1998).

Neuroscientific investigations of priming have most often revealed reductions in activity, measured at the level of neuronal activity in nonhuman primate recording (Li et al. 1993; Miller et al. 1991) and aggregate measures of neural activity based on hemodynamics in humans (Buckner et al. 1995, 1998a; Demb et al. 1995; Dobbins et al. 2004; Henson 2003; Henson et al. 2000; Schacter and Buckner 1998; Schacter et al. 1996; Squire et al. 1992; van Turennout et al. 2000; Wagner et al. 1997; Wig et al. 2005). Importantly, although the precise neurophysiological mechanisms that mediate these changes remain unclear (for review see Grill-Spector et al. 2006), recent studies have linked the neural changes, referred to as *repetition suppression* or *neural priming*, to the behavioral changes (i.e., *behavioral priming*) using both correlational methods in neuroimaging studies (e.g., Dobbins et al. 2004; Lustig and Buckner 2004; Maccotta and Buckner 2004; Turk-Browne et al. 2006; for review see Schacter et al. 2007) and transient cortical disruption (Wig et al. 2005).

Behavioral priming is known to involve multiple component processes. Given the same initial experience, repetition can have distinct effects on later perceptual processing of the item (perceptual priming) as well as amodal processing of abstract or semantic features of the item (conceptual priming). The distinction between perceptual and conceptual priming has been supported by behavioral dissociations. For example, changes in stimulus format across repetitions can reduce priming effects on tasks that demand detailed analysis of the stimulus format, while having little effect on tasks that demand semantic categorization (Blaxton 1989; Roediger 1990; Roediger and Blaxton 1987). These distinctions have raised the possibility that a single experience can simultaneously influence multiple systems and modules responsible for information processing (Henson 2003; Schacter 1992; Schacter et al. 2007; Tulving and Schacter 1990).

Convergent methods provide support for the idea that priming may arise from distinct influences on multiple brain systems. Studies of patients with focal brain lesions have demonstrated deficits in form-specific perceptual priming following damage to right-occipital cortices (Gabrieli et al. 1995). Functional neuroimaging investigations in healthy young adults have revealed sensitivity of visual regions to perceptual manipulations and have suggested a processing gradient such that neural priming is maintained across more extensive stimulus transformations as one moves along the visual processing hierarchy (e.g., luminance, viewpoint, position, size, shape, and object), and even across homologous regions from right-to-left hemispheres (for review see Schacter et al. 2007). It has been suggested that changes in processing efficiency are associated with a "sharpening" or "tuning" of the neuronal responses within cortical areas that represent perceptual attributes of the stimulus (Desimone 1996; Wiggs and Martin 1998).

In parallel, functional neuroimaging research investigating semantic or conceptual processing (e.g., semantic classification, generation, or naming) has revealed that repetition-mediated facilitation in this domain may be related to operations supported by frontal and temporal regions. Modifications across regions of the inferior frontal gyrus, and inferior- and middle-temporal gyri have been linked to increased fluency in

Address for reprint requests and other correspondence: G. S. Wig, Harvard University, Department of Psychology, 33 Kirkland Street, Cambridge, MA 02138 (E-mail: gwig@wjh.harvard.edu).

the retrieval of semantic information that accompanies repetition (Buckner et al. 1998a, 2000; Demb et al. 1995; Thompson-Schill et al. 1999; van Turennout et al. 2000; Wagner et al. 1997, 2000; Wig et al. 2005). It has been suggested that these effects are distinct from the perceptually driven effects discussed earlier and likely reflect abstract processing of lexical or semantic attributes. Moreover, neuropsychological testing of patients with Alzheimer's disease (Fleischman and Gabrieli 1998; Keane et al. 1991) has uncovered priming deficits preferential to conceptual processing, consistent with a distinct locus of effect.

Along these lines, more recent research has highlighted a component of priming that is related to the particular response or decision that a participant makes about a target item. Inversion of the classification-task between study and test sessions (e.g., judging whether an item is "bigger than a shoebox" during study and then whether it is "smaller than a shoebox" at test) has been found to attenuate both behavioral priming and neural priming in frontal, fusiform, and extrastriate regions (Dobbins et al. 2004). Importantly, when the classification task is restored to the original format, behavioral priming and neural priming in these regions reemerge. These findings indicate that neural priming can be sensitive to the exact decision made about the target item (Logan 1990).

Collectively, these results raise the possibility that the same initial experience can have multiple effects at different stages of information processing from perception to decision. Here, using manipulations of stimulus and decision types, we adopt an experimental functional magnetic resonance imaging (fMRI) paradigm aimed at simultaneously dissociating regions that mediate priming across perceptual (i.e., changes across stimulus format independent of the abstract level of representation or decision) and conceptual dimensions.[1] As the results will reveal, separate regions are preferentially sensitive to these distinct dimensions, supporting the hypothesis that the same exposure can simultaneously have multiple neural effects. In a second analysis, we use functional connectivity MRI (fcMRI) during resting scans to show that the regions differentially affected by manipulations of perceptual and conceptual processes are embedded within distinct brain systems.

We used an experimental paradigm that allowed us to examine, within a single task, multiple dimensions of both behavioral priming and neural priming. During the initial study session, participants performed a semantic classification decision on a set of repeating colored objects (see *Task procedures*). Following this initial exposure, participants were scanned using fMRI during a test session that held constant or changed the task decision (Fig. 1*A*) and/or stimulus format (Fig. 1*B*). By crossing changes in decision and stimulus format, we were able to dissociate and reveal the nature of processing within distinct brain systems during repetition priming.

[1] Throughout this article, we distinguish perceptual from conceptual priming/processing, consistent with prior usage in the priming literature (e.g., Keane et al. 1991; Roediger 1990). Note that our use of the term "conceptual priming" does not imply a commitment to the idea that behavioral or neural priming solely reflects a change in the representation of conceptual knowledge, but rather encompasses both the changes in the representation of conceptual knowledge as well as changes in processes used to gain access to that knowledge.

METHODS

Participants

Participants were recruited from the local Boston community. All participants were right-handed, native speakers of English, reported no significant abnormal neurological history, and had normal or corrected-to-normal visual acuity. Participants were paid for their participation and gave informed consent in accordance with the guidelines set by the Human Subjects Research Committee at Massachusetts General Hospital and Harvard University.

Thirty-three participants were scanned in the main experiment. Of the 33 participants, 3 participants did not show a behavioral measure of priming during the study session (defined here as a difference of response time that is >0 ms when comparing first and third repetitions of object classifications), and 3 participants failed to provide a behavioral response to an excessive number of trials (i.e., number of "no responses" $>10\%$ of total trials). Because these participants could be considered noncompliant to experiment instructions (failing to demonstrate behavioral priming under conditions that have consistently demonstrated robust indices of response facilitation following repetition, or failing to provide an adequate number of responses), they were excluded from the experimental analysis. The behavioral and functional data reported here reflect the remaining 27 participants (15 female; mean age = 23 yr; range of age 18–30 yr).

A second data set was used in a formal replication analysis of resting-state correlations. Twenty-four participants were scanned for this replication data set (13 female; mean age = 23 yr; range of age 18–35 yr).

Apparatus

All imaging was performed on a 3T Siemens Magnetom TimTrio Scanner (Siemens Medical Solutions, Erlangen, Germany), equipped with a 12-channel head coil at the Athinoula A. Martinos Center for Biomedical Imaging, Massachusetts General Hospital (Charlestown, MA). Visual stimuli were presented using an Apple Powerbook G4 Laptop computer running Matlab 7.1 using the psychophysics toolbox extensions (Brainard 1997). Stimuli were projected to participants with a JVC (model SX21/s) D-ILA projector onto a screen positioned at the head end of the bore. Participants viewed the screen through a mirror mounted on the head coil. Cushions and clamps were used to minimize head movement.

Imaging

Anatomical images were acquired using a high-resolution three-dimensional magnetization-prepared rapid gradient echo sequence (MPRAGE; 128 sagittal slices, echo time [TE] = 3.39 ms, repetition time [TR] = 2,530 ms, flip angle = 7°, voxel size = 1 × 1 × 1.33 mm). Functional data were collected in four runs using T2* gradient echo, echo planar imaging (EPI) sensitive to blood oxygen level–dependent (BOLD) contrast (TR = 2,500 ms, TE = 30 ms, flip angle = 90°, 3 × 3-mm in-plane resolution: 174 sets of images). Slices were acquired axially, allowing whole brain coverage, and were tilted parallel to the anterior commissure–posterior commissure plane (36 slices; 3-mm slice thickness, 0.5-mm skip between slices).

Stimulus materials

The stimuli consisted of 360 color picture pairs; the picture pair set was an updated version of one used in previous research (Koutstaal et al. 2001; Simons et al. 2003). The picture pairs depicted single man-made or living objects (e.g., anchor, shark; see Fig. 1*B*), with the items in each pair representing perceptually different exemplars of objects with the same name.

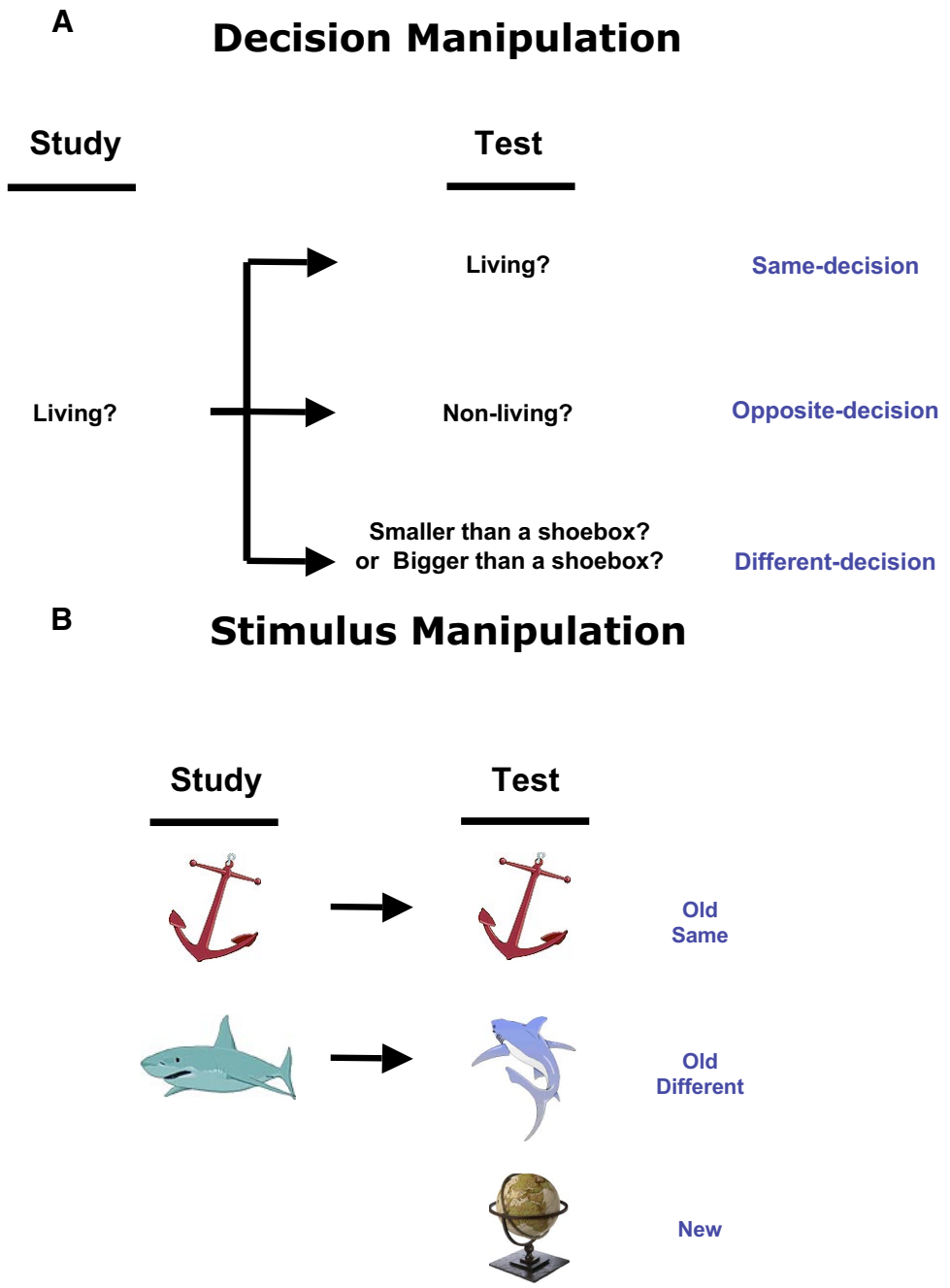

FIG. 1. Experiment manipulations. Participants initially made a semantic classification on a repeating set of colored objects (study session). This study session was followed by a test session. *A*: at test, participant's performed 3 separate semantic classifications on independent sets of objects (decision manipulation): the same-decision as that performed at study, the opposite-decision as that performed at study, and a different-decision as that performed at study. *B*: within each decision, participants made classifications on old objects and new objects (stimulus manipulation). The old objects were either the same object as that classified at study (old-same) or same name exemplars (old-different) of previously classified objects.

Task procedures

Before being placed in the MRI scanner, participants were given a description of the task procedures and presented with examples of colored objects and task-instruction screens similar to those that they would be viewing.

PRACTICE SESSION. While in the MRI scanner, participants were first given a practice session (functional data were not collected during this practice period). During this practice session, participants performed a semantic classification task (yes/no) on a set of 50 colored objects. These colored objects were different from the set of 360 color picture pairs used in subsequent parts of the experiment. The specific semantic classification decision was the same as that which would be made during the subsequent study sessions. An instruction screen preceded the object set; this instruction screen was presented for 5 s, indicating which classification task was to be performed, and depicted a figure reminding participants of the finger-to-response mapping. All responses were made using a button-box placed in the participant's left hands (yes and no responses were made using participant's pointer and middle fingers, respectively). Both the response-hand and finger-to-response mapping remained the same across the entire experiment and was the same for each participant. Participants were told to make the classification decision as quickly as possible, without sacrificing accuracy. Each object was presented individually at the center of the screen for 500 ms, at a rate of one every 2,500 ms. A centrally presented black fixation crosshair was presented during the 2,000-ms interstimulus interval. Objects were each presented once during this practice session. This practice session served two main purposes: it familiarized participants with the semantic classification procedure and also familiarized participants with the decision they would be making throughout the subsequent study sessions.

STUDY SESSION. Following the practice session, participants performed a study session. Participants made a semantic classification on a set of 60 colored objects. A 5-s instruction screen indicating the specific decision to be made preceded the presentation of objects. The 60 objects were each presented three times in random order, for a total of 180 trials. Each object was presented individually at the center of the screen for 500 ms, at a rate of one every 2,500 ms. A centrally presented black fixation crosshair was presented during the 2,000-ms interstimulus interval.

The classification decision used in the study sessions was randomly selected from one of four semantic classifications for each participant, and remained the same across all study sessions. *1*) "Is this object living?" *2*) "Is this object nonliving?" *3*) "Is this object smaller than a shoebox in real life?" *4*) "Is this object larger than a shoebox in real life?"

TEST SESSION. A test session followed the study session. At test, processing was manipulated along dimensions of decision and stimulus types. During the test session, participants alternated between blocks of fixation (i.e., passive rest) and blocks of task (semantic classification). During blocks of fixation (25 s; 10 TRs), participants were presented with a centrally presented black fixation crosshair and were instructed to simply fixate on this crosshair. Blocks of task (112.5 s; 45 TRs) followed blocks of fixation and began with the presentation of an instruction screen lasting 5 s (2 TRs) in duration. This instruction screen indicated which classification decision was to be performed on the objects that followed and depicted a figure reminding participants of the finger-to-response mapping. Participants made the semantic classification indicated by the instruction screen on a set of 30 colored objects that followed. As in the practice and study sessions, each object was presented individually at the center of the screen for 500 ms, at a rate of one every 2,500 ms (1 TR). A centrally presented fixation crosshair was presented during the 2,000-ms interstimulus interval. Further, these object-classification trials were interleaved with periods of fixation, varying in duration from 0 to 10 s (0–4 TRs; 15 TRs interleaved in total per block of task). This "jittering" of periods of fixation within each task block allowed for simultaneous estimation of both "transient" (event-related) and "sustained" test session BOLD signals (see FMRI-STATISTICAL IMAGES AND REGION OF INTEREST ANALYSIS in the following text) and was optimized for hemodynamic response estimation efficiency using optseq2 (http://surfer.nmr.mgh.harvard.edu/optseq/). The focus of this study will be on these former, transient responses. Crosshairs that were presented during the task periods were red in color, to differentiate them from the black crosshairs presented during blocks of fixation, thus serving as a cue to remind participants that they were presently in a task block. Task blocks concluded with an instruction screen that stated that the present task was complete (presented for 2.5 s; 1 TR). The test session concluded with a block of fixation to allow for adequate recovery of the hemodynamic response following the last task block. As such, the test session was 435 s in duration (174 TRs).

Within each test session, a decision manipulation was imposed such that participants performed three different decisions across the three task blocks of a given test session run (Fig. 1*A*). *1*) the same classification decision as that which was performed during the study session (same-decision; e.g., "Is this object Living?"), *2*) the same classification decision but requiring the opposite response along the same dimension judged at study (opposite-decision; e.g., "Is this object Nonliving?"), and *3*) a classification task with a dimension of classification that was orthogonal to that of the study period classification task (different-decision; e.g., "Is this object smaller than a shoebox in real life?" or "Is this object bigger than a shoebox in real life?"). Decision types were presented in random order and the different-decision alternated across each test session for every participant such that half the different-decisions were of one classification question (e.g., "Is this object smaller than a shoebox in real life?"), whereas the other half were of the opposite classification question (e.g., "Is this object bigger than a shoebox in real life?").

The stimulus manipulation was such that participants viewed both novel and old objects within each task block (30 objects total). Old objects were either the exact same objects as those previously classified during the study session (old-same) or different exemplars of objects previously classified during the study session (old-different; Fig. 1*B*). As such, within each task block, participants viewed three types of object stimuli: objects previously classified during the study session (old-same; 10 objects), different exemplars of previously classified objects (old-different; 10 objects), and objects that had not been classified during the study session (new; 10 objects). Objects were never repeated within the test sessions and object/exemplar pairs were never reused across task conditions.

Importantly, all decision and stimulus lists were systematically counterbalanced and randomized between participants, to minimize any potential confounds of classification decision, stimulus list, presentation order, or any interaction between these variables. Participants completed a total of four sets of the study-test sessions.

REST FIXATION SCANS. A subset of individuals ($n = 20$) underwent two additional fMRI scans to acquire data for analysis of resting-state functional connectivity. These additional two scans flanked the beginning and end of the repetition-priming experiment so as not to alter the nature of the experimental paradigm in any manner across participants. During each of these two additional scans, participants were instructed to simply fixate a centrally presented black fixation crosshair for the duration of the scan. Each scan lasted 310 s (124 TRs). Participants were asked to stay awake and alert throughout the duration of each of these scans.

Data analysis

FMRI-PREPROCESSING OF FUNCTIONAL IMAGES. fMRI test session data were analyzed using SPM2 (Wellcome Department of Imaging Neuroscience, London, UK) (Friston et al. 1995). For each functional run, data were preprocessed to remove sources of noise and artifact. The first four volumes (10 s) of each run were excluded from analyses to account for T1 saturation effects. Preprocessing included slice-time correction to correct for differences in acquisition time between slices for each whole brain volume; realignment within and across runs to correct for head movement; unwarping to correct for susceptibility-by-movement interactions ("field-disturbances"); normalization to a standard anatomical space (3-mm isotropic voxels) based on the SPM2 EPI template, which approximates the atlas space of Talairach and Tournoux (1988); and spatial smoothing (6-mm full-width at half-maximum [FWHM]) using a Gaussian kernel.

FMRI-STATISTICAL IMAGES AND REGION OF INTEREST ANALYSIS. Preprocessed data were analyzed using the general linear model. Analysis was performed to separate transient from sustained signal changes while accounting for nuisance covariates of no interest (Chawla et al. 1999; Donaldson et al. 2001). These variables of no interest included session means, linear trends to account for low-frequency noise (scanner drift), and six movement parameters obtained from realignment. Because the aims of the experiment were to interrogate item-by-item repetition-related changes (neural priming) across decision and stimulus manipulations, the description of the subsequent analysis will focus on the transient (event-related) signals.

For each participant, the BOLD response to each trial type [i.e., responses associated with presentation of old-same, old-different, and new items within each decision manipulation (same-decision, opposite-decision, different-decision); 9 in total] was estimated by coding a different regressor for each of the seven time points (i.e., image acquisitions) immediately after each stimulus onset. This was implemented in SPM2 using a "finite impulse response" (FIR) function. FIR regressors were also coded to account for the instruction screen at the

beginning and end of the task block to account for block transitions (Konishi et al. 2001). As such, this estimation produced seven parameter estimates (corresponding to the seven time points, or 17.5 s poststimulus onset) per voxel per condition (11 conditions total).

Based on the anticipated temporal profile of the peak BOLD response (Miezin et al. 2000), parameter estimates corresponding to 2.5 to 10 s poststimulus onset (time points 2, 3, and 4) were carried forward into subsequent analysis. For each participant, a weighted-parameter estimate was computed for each of these three time points. This estimate identified voxels demonstrating greater activity during classification of new objects relative to old objects (collapsed across all decision conditions (same-decision, opposite-decision, different-decision) and old object types (old-same, old-different)). As such, each of these weighted-parameter estimates reflected repetition-related reductions (neural priming) independent of the task and stimulus manipulations. These individual contrast images were next submitted to a random-effects analysis, treating participant as the random factor, to create statistical activation maps using a one-sample *t*-test. A combined statistical map was created by applying a voxel-by-voxel search algorithm on each of the three *t*-maps. This algorithm collapsed the three statistical maps (one for each of the three time points of interest) into a single *t*-map by assigning each voxel to a value equivalent to the maximum *t*-value identified among the three individual maps. As such, this map reflected the maximum *t*-value of a given voxel (peak), independent of its temporal lag[2] (Buckner et al. 1998b; Schacter et al. 1997). This final *t*-map was used in subsequent region of interest (ROI) definition. An automated search algorithm identified the peak coordinate locations and all surrounding voxels (8-mm ROI sphere radius) that surpassed a $P = 0.005$ threshold.[3]

Inspection of the full hemodynamic temporal profile (7 time points; from 0 to 17.5 s poststimulus onset) of the region containing the global maxima of this *t*-map (right middle occipital gyrus; R MOG; BA 19; peak *x y z* Talairach and Tournoux atlas coordinates: 39 −83 21) revealed that the peak BOLD response occurred during time points 2 and 3, corresponding to 2.5–5 and 5–7.5 s poststimulus onset, respectively. Subsequent statistical analyses were focused on the average weighted-parameter estimates derived from these two time points.

Motivated by a review of the literature on neural priming (Schacter et al. 2007), specific peaks of interest associated with neural priming were selected a priori from previous published studies from our laboratories. This was achieved by calculating the average peak coordinate in the "x," "y," and "z" planes across each respective study for a given region. Regions associated with stimulus-to-decision mapping and conceptual priming were defined around peak locations at *1*) left posterior-inferior frontal gyrus (L pIFG; Brodmann area [BA] 44), *2*) right posterior-inferior frontal gyrus (R pIFG; BA 44), *3*) left anterior-inferior frontal gyrus (L aIFG; BA 47), and *4*) left middle temporal gyrus (L MTG; BA 21). Regions associated with perceptual priming were centered on *1*) left inferior temporal gyrus/fusiform gyrus (L ITG-FG; BA 21/37) and *2*) right inferior temporal gyrus/fusiform gyrus (R ITG-FG; BA 21/37). Table 1 provides a summary of the regions, the studies that were used to identify peak coordinates for these regions, and the computed average peak coordinates.

The final step in ROI definition involved identification of the closet peak voxel from the final *t*-map to each precalculated average region peak (from Table 1). Table 1 reveals the proximity between obtained and calculated peak coordinates. Critically, this method allowed us to include only those voxels that surpassed the given threshold that surrounded our obtained peaks when constructing ROIs. The exception to this ROI selection procedure was for ROIs within the left inferior-temporal gyrus (L ITG-FG) and anterior portion of the left inferior frontal gyrus (L aPFC) because the search algorithm failed to produce peak coordinates in close proximity to our precalculated peaks. Spherical ROIs were constructed around these regions (6-mm radius). The L ITG-FG ROI did not overlap with the L MTG ROI. For each ROI, mean parameter estimates for each transient trial type of interest [separated by stimulus (old-same, old-different, new) and decision (same-decision, opposite-decision, different-decision)] were extracted.

An advantage to this approach is that it allows for integration of theoretically motivated region selection (i.e., "top-down," based on previous data) with the informational content of the data set that is to be ultimately interrogated (i.e., "bottom-up," based on the data set of interest). One caveat to this approach is that ROI selection was biased toward identifying voxels that exhibited significant neural priming across all conditions. Accordingly, caution is warranted when interpreting parameter estimates of the absolute level of neural priming; as such, we place greater emphasis on differences in neural priming across conditions as opposed to the presence or absence of neural priming in any particular condition, per se.

Resting-state functional connectivity analysis

Following preprocessing of the functional images, several additional steps described in previous studies (Fox et al. 2005; Vincent et al. 2006) were taken to prepare the rest fixation-scan data set (two functional runs collected in 20 of the participants) for resting-state functional connectivity MRI (rs-fcMRI) analysis. First, low- and high-frequency components of the atlas-aligned BOLD data were removed using a temporal band-pass filter retaining $0.009 \text{ Hz} < f < 0.08 \text{ Hz}$. Next, data were spatially smoothed using a Gaussian kernel of 6 mm FWHM. Removal of several spurious or nonspecific sources of variance was accomplished by regression of the following variables: *1*) the six movement parameters computed by rigid body

[2] As opposed to using the maximum parameter estimate across the three time bins (hemodynamic lags), an alternative approach to this method would have been to average across the time bins, although this would have reduced the value of the estimates.

[3] This statistical threshold was set to improve the likelihood that the search algorithm would identify peak voxels proximal to our a priori defined ROIs (Table 1). Importantly, this search was implemented on a whole brain neural priming map that was statistically orthogonal to experimental manipulations (changes in task and material types) that were tested in ROI analysis.

TABLE 1. *Regions of interest (ROIs)*

Regions	Approximate Gyrul Location	Brodmann's Area	Reference(s)	Average Atlas Coordinates			ROI Peak Coordinates		
				x	y	z	x	y	z
L pIFG	Left posterior inferior frontal gyrus	44	Dobbins et al. (2004); Wig et al. (2005)	−45	10	24	−42	7	25
R pIFG	Right posterior inferior frontal gyrus	44	Koustaal et al. (2001); Simons et al. (2003)	45	7	27	50	4	27
L aIFG	Left anterior inferior frontal gyrus	47	Wagner et al. (2000); Wig et al. (2005)	−48	26	1	*		
L ITG-FG	Left inferior temporal gyrus/fusiform gyrus	21/37	Koustaal et al. (2001); Simons et al. (2003)	−45	−53	−10	*		
R ITG-FG	Right inferior temporal gyrus/fusiform gyrus	21/37	Koustaal et al. (2001); Simons et al. (2003)	48	−59	−7	48	−50	−8
L MTG	Left middle temporal gyrus	21	Buckner et al. (2001); Wig et al. (2005)	−56	−52	0	−47	−52	0

*Spherical ROI (6-mm radius) centered around region's average atlas coordinates (see text for details).

translation and rotation in preprocessing, *2*) the mean whole brain signal, *3*) the mean signal within the lateral ventricles, and *4*) the mean signal within a deep white matter ROI. The first temporal derivative of each time course was also included in the regression procedure to account for temporally shifted nuisance waveforms. Regression of each of these signals was computed simultaneously and the residual time course was retained for the following correlation analysis.

Four separate exploratory correlation analyses were performed to yield rs-fcMRI correlation maps between a seed region and all voxels across the whole brain. The seed regions were selected from the ROIs of the task-evoked functional data set: L pIFG (BA 44), the R MOG global maxima obtained from the collapsed group neural priming map (Fig. 3), L ITG-FG (BA 21/37), and L MTG (BA 21). For each participant, the average time course was extracted from the region and a correlation coefficient was computed between this seed region's time course and the time course for each voxel across the whole brain using Pearson's product-moment formula. The resulting correlation map was converted to z values using Fisher's *r*-to-z transformation (Zar 1996). The individual z(*r*) images were next submitted to a random-effects analysis, treating participant as the random factor, to create statistical activation maps using a *t*-test ($P < 0.001$). A more conservative analysis was used for rs-fcMRI maps because these were considered more exploratory in nature. To confirm the results of this analysis, a formal replication analysis was conducted using an independent data set (see the following text).

Resting-state functional connectivity replication analysis

To test for replication across independent data sets and to demonstrate the presence of distinct systems, resting period data were collected from an additional 24 participants ("group B") using scanning parameters identical to those of the original sample ("group A"). Analyses were implemented in two steps: *1*) Hypothesis generation to identify target regions of interest in group A and *2*) Hypothesis testing of whether the correlation patterns replicated using the independent data set (group B).

Hypothesis generation entailed identification of regions that were functionally correlated with L MTG and L ITG-FG seed regions within group A (i.e., Fig. 8). Correlations with regions of the left inferior frontal gyrus (L IFG) and right middle occipital gyrus (R MOG) were the primary focus given these region's roles in conceptual and perceptual operations, respectively, and were previously highlighted as nodes in distinct systems (see Figs. 6 and 8). L IFG and R MOG target regions of interest were identified by first computing two independent sets of resting-state correlation maps: one using the L MTG seed and one using the L ITG-FG seed. Each map was examined at a threshold of $P < 0.001$, uncorrected (i.e., Fig. 8). The L IFG target ROI was obtained from the resting correlation map using the L MTG seed (Fig. 8, red). The R MOG target ROI was obtained from the resting correlation map using the L ITG-FG seed (Fig. 8, green). We hypothesized that temporal regions would be functionally linked to systems recruited during conceptual/semantic and perceptual processing. Accordingly, we did not restrict ROI definition to a subset of voxels within frontal and occipital cortices because different elements of semantic processing have been linked to the extent of L IFG across pars triangularis and pars opercularis of the left hemisphere (for review see Badre and Wagner 2007) and the middle-occipital gyrus is considered to be visually responsive unimodal cortex based on its anatomical connectivity and functional characteristics (Felleman and Van Essen 1991; Ungerleider 1995). Thus all clusters within the L IFG (BA 44, 45, and 47) and R MOG (BA 19) surviving the threshold were combined to produce the target ROIs.

The second independent data set was used for hypothesis testing (group B). All preprocessing of rest fixation scan data was identical to that previously described for the group A rest data. Two independent resting-state correlation maps were produced: one using the L MTG seed and one using the L ITG-FG seed. To determine the strength of correlations between seed regions and the target ROIs, the independently defined L IFG and R MOG ROIs obtained from the hypothesis generation analysis (group A) were probed in the group B data set. The mean z(*r*) values of each of these regions were extracted from each correlation analysis and submitted to a two-way ANOVA including factors of seed (L MTG and L ITG-FG) and target (L IFG and R MOG), and followed up with planned comparisons.

RESULTS

Behavioral

All statistical analyses of behavioral data were performed on participants' median response times during semantic classification. For each decision during the test sessions (same-decision, opposite-decision, different-decision), median response times were calculated for each stimulus type (old-same, old-different, new). Within each decision, behavioral priming scores were calculated for each stimulus type as the average difference in response time between new and old objects: new minus old-same and new minus old-different. These scores reflect the benefit in response time that was afforded to stimulus repetition within each decision as a function of whether the repetition was the same object or a different exemplar of an object previously classified during the study session.

A two-way repeated-measures ANOVA was conducted to examine the main effects of decision (same-decision, opposite-decision, different-decision), stimulus (old-same and old-different), and their interaction on the behavioral measure of priming across participants. The statistical test revealed a significant main effect of decision [$F(2,52) = 6.62$, $P < 0.005$], a trend toward main effect of stimulus [$F(1,26) = 3.17$, $P = 0.09$], but no significant interaction between the two ($P = 0.41$; Fig. 2).

Follow-up planned comparisons demonstrated that greater behavioral priming resulted from performance of the same-decision compared with both the opposite- and different-decisions, independent of the material type [same-decision > opposite-decision: $t(53) = 2.29$, $P < 0.05$; same-decision > different-decision: $t(53) = 5.53$, $P < 0.001$], whereas performance of the opposite- versus different-decision resulted in a statistically nonsignificant trend toward greater priming [opposite-decision > different-decision: $t(53) = 1.91$, $P = 0.06$].

Consistent with previous demonstrations of response learning (Dobbins et al. 2004; Schnyer et al. 2007), behavioral priming was significantly greater during classification of old objects while participants performed the same-decision relative to classification of old items when the response was opposite as that required during the study session [i.e., the opposite-decision; $t(26) = 2.27$, $P < 0.05$]. Further, this pattern of significantly greater behavioral priming was also observed when comparing behavioral priming during classification of old-same objects relative to classification of old-different objects during the same-decision [new minus old-same > new minus old-different: $t(26) = 3.27$, $P < 0.005$]. Together, these data highlight the sensitivity of behavioral measures of repetition priming to stimulus-to-decision mapping; although not always eliminated, behavioral priming is reduced following changes to either the stimulus type or the decision type (but also see Supplemental Results and Supplemental Fig. S1).[4]

[4] The online version of this article contains supplemental data.

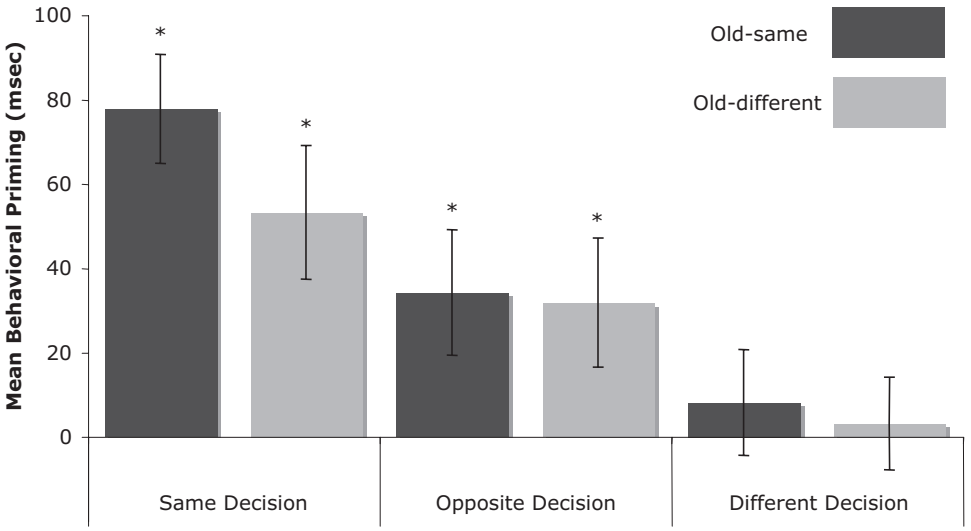

FIG. 2. Test period behavioral priming is sensitive to manipulations of decision and stimulus types. Participants' mean behavioral priming scores during the test period. Behavioral priming was calculated as a difference in median response times between new and old objects for each decision type (same-decision, opposite-decision, different-decision) and stimulus type (old-same and old-different). Error bars correspond to the SE. *One-sample *t*-test denoting significant behavioral priming at an alpha of 0.05.

Functional neuroimaging

TASK-EVOKED BOLD FMRI DATA. Consistent with previous research, neural priming during the test period was observed in a number of regions including bilateral regions of the inferior frontal gyrus, middle- and inferior-temporal gyri, fusiform gyrus, and occipital cortices (Fig. 3). The statistical analysis identified voxels demonstrating significantly greater BOLD activity during classification of new objects relative to classification of old objects, collapsed across all decision and stimulus manipulations, and was subsequently used to guide the ROI analysis (see following text).

To ensure that the subsequent ROI analysis was performed in an unbiased manner, ROI definition was conducted using a two-step "guided" ROI procedure. A priori regions were initially identified based on peaks of interest from prior literature (Table 1) and localized in the present data set using the neural priming statistical activation map that collapsed data across all conditions (Fig. 3). Statistical interrogation of the mean BOLD parameter estimates for each condition was then performed using these ROIs defined independent of condition effects.

This hypothesis-driven analysis focused on regions of the left (BA 44 and BA 47) and right (BA 44) inferior frontal

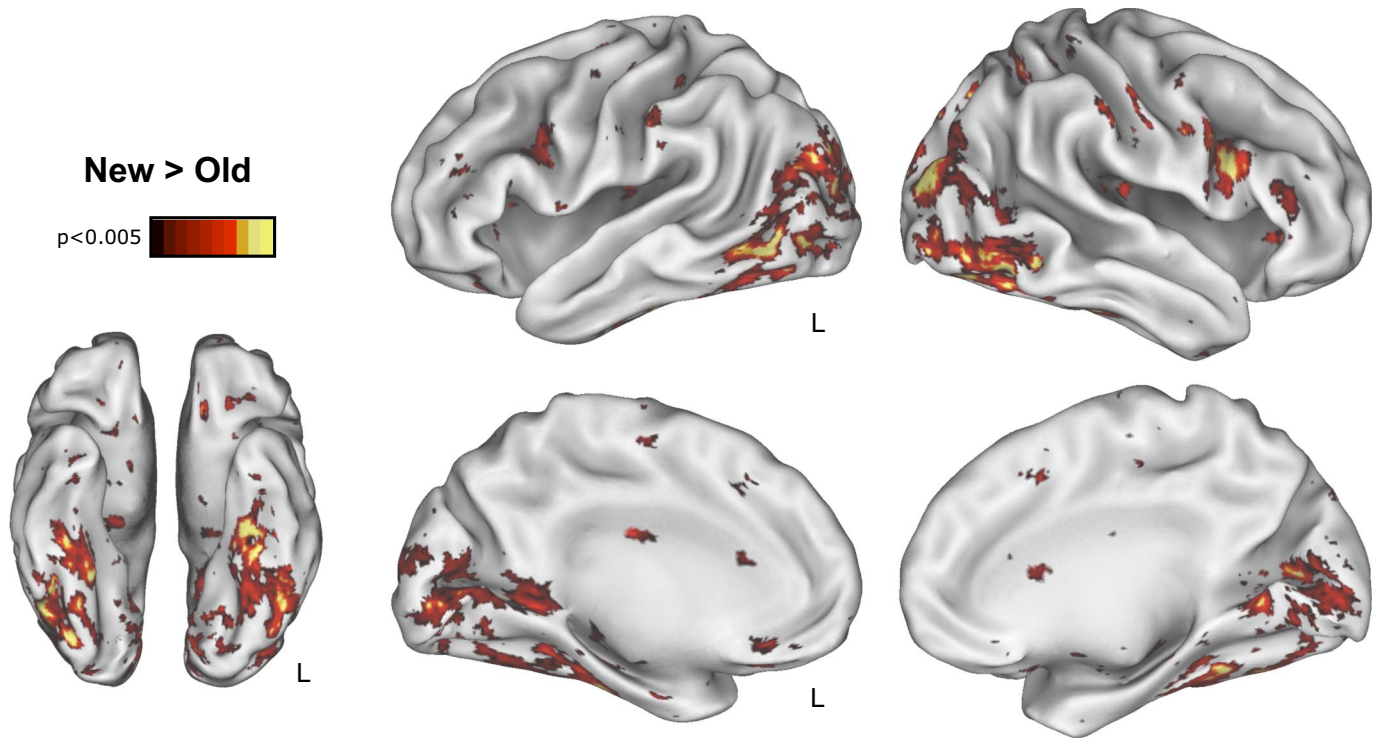

FIG. 3. Whole brain test period neural priming. Whole brain group statistical activation map comparing new to old items ($P < 0.005$, uncorrected) overlaid on partially inflated cortical renderings of the left and right hemispheres using cavet software (Van Essen, 2005). Analysis is collapsed across the decision manipulation (same-decision, opposite-decision, different-decision) and old stimulus types (old-same and old-different). Among other regions, significant neural priming was observed within bilateral regions of the inferior frontal gyrus (IFG), inferior- and middle-temporal gyri (ITG and MTG, respectively), fusiform-gyrus (FG), and occipital cortex. This whole brain analysis was used to guide subsequent region of interest (ROI) selection (see text for details). *Top*: lateral views of the left and right hemispheres. *Bottom*: ventral and medial views of the left and right hemispheres.

gyrus, left middle temporal gyrus (BA 21), and left and right inferior temporal gyrus/fusiform gyrus (BA 21/37). Previous research has implicated each of these regions in demonstrating decision and/or stimulus specificity within paradigms exploring repetition priming and semantic classification.

Mirroring the behavioral priming analysis, fMRI (BOLD) ROI data were analyzed to explore the effect of manipulations of decision type (Fig. 1*A*) and stimulus type (Fig. 1*B*) on repetition-related reductions, calculated as the mean difference in parameter estimates between new and old objects (i.e., neural priming or repetition suppression).

Participants' neural priming scores from homologous ROIs of the posterior inferior frontal gyrus (pIFG; BA 44) were submitted to a three-way repeated-measures ANOVA, incorporating the effects of hemisphere (left and right), decision (same-decision, opposite-decision, and different-decision), and stimulus priming (new minus old-same and new minus old-different). Results from the ANOVA revealed no main effects of hemisphere [$F(1,26) = 0.14$, $P = 0.71$], decision [$F(2,52) = 1.77$, $P = 0.18$], or stimulus [$F(1,26) = 1.13$, $P = 0.30$], but did show a decision $\times$ stimulus interaction [$F(2,52) = 3.50$, $P < 0.05$; Fig. 4*A*]. No other interactions were significant (all $P > 0.27$). Collapsing across the hemispheres, planned comparisons of neural priming scores revealed a pattern mimicking the pattern observed when examining participants' behavioral priming scores: neural priming of old-same objects (new minus old-same) was significantly greater while performing the same-decision relative to classification during either of the other two decision conditions [same-decision $>$ opposite-decision: $t(53) = 3.13$, $P < 0.005$; same-decision $>$ different-decision: $t(53) = 2.86$, $P < 0.01$]. Neural priming was also greater for old-same objects relative to old-different objects, but only when participants were engaged in the same-decision [new minus old-same $>$ new minus old-different: $t(53) = 3.31$, $P < 0.005$]. Examining the effects of decision and stimulus on neural priming within the left anterior inferior frontal gyrus ROI (BA 47) failed to reveal any statistically significant main effects or interactions (all $P > 0.12$) and significant neural priming was not observed under any condition (all $P > 0.12$).

In contrast to frontal regions, the ROIs within the inferior temporal gyrus/fusiform gyrus (ITG-FG; BA 21/37) demonstrated sensitivity to the stimulus type independent of the decision that was made. A three-way repeated-measures ANOVA, incorporating effects of hemisphere (left and right), decision (same-decision, opposite-decision, and different-decision), and stimulus priming (new minus old-same and new minus old-different) demonstrated no effect of hemisphere [$F(1,26) = 0.17$, $P = 0.68$] or decision [$F(2,52) = 0.094$, $P = 0.91$], a main effect of stimulus type [$F(1,26) = 6.07$, $P < 0.05$], and no significant interactions (all $P > 0.25$). Collapsing across the hemispheres and decisions, planned comparisons revealed that greater neural priming was associated with classification of old-same objects relative to classification of old-different objects [new minus old-same $>$ new minus old-different: $t(161) = 3.48$, $P < 0.001$; Fig. 4*B*].

To further examine these observations and determine whether frontal and inferior-temporal ROIs did indeed demonstrate reliably different patterns of neural priming effects across the manipulations, a three-way ANOVA incorporating region [pIFG (collapsed across hemispheres) and ITG-FG (collapsed across hemispheres)], decision (same-decision, opposite-decision, different-decision), and stimulus priming (new minus old-same and new minus old-different) was conducted. Analysis revealed a significant region $\times$ decision $\times$ stimulus interaction [$F(2,106) = 3.34$, $P < 0.05$], confirming the differential sensitivity of frontal and inferior-temporal regions to manipulations of decision type and stimulus type.

Statistical interrogation of the ROI situated within the left middle temporal gyrus (MTG; BA 21) revealed that this region failed to demonstrate significant differences across decision or stimulus types when interrogated in an ANOVA model (all main effects and interactions, $P > 0.48$). Unlike pIFG and ITG-FG ROIs, however, neural priming was observed in all conditions (all $P < 0.05$; Fig. 5). As previously noted, these results should be interpreted with caution because ROI selection was guided by a statistical map that might be considered biased in its identification of voxels demonstrating neural priming.

RESTING-STATE FUNCTIONAL CONNECTIVITY ANALYSIS. Analysis of the task-evoked activity revealed a functional-anatomical dissociation between priming effects across the ROIs. Whereas neural priming in regions of the left and right pIFG demonstrated sensitivity to the decision type and stimulus type, neural priming in the left and right ITG-FG was insensitive to manipulations related to the decision made on the object but was sensitive to the stimulus manipulation, demonstrating stimulus specificity.

The results suggest that these regions may be embedded within distinct brain systems differentially involved in conceptual and perceptual processing, respectively. The anatomic locations of the regions are consistent with this hypothesis. To explicitly explore whether the regions are components of dissociable brain systems, we used resting state functional connectivity MRI (rs-fcMRI), which allows brain systems to be identified based on intrinsic, low-frequency correlations between brain regions. We hypothesized that the regions showing differential effects are part of distinct brain systems. For this analysis, a subset of the participants ($n = 20$) was scanned during two extended periods (5 min each) of awake resting fixation. rs-fcMRI has proven to be robust using these parameters (for review see Fox and Raichle 2007).

rs-fcMRI analysis was first focused on the L pIFG as a "seed region" of interest. Task-evoked activity within this region during the repetition priming paradigm revealed its sensitivity to stimulus-to-decision mapping: this region was sensitive to changes in the mapping of a specific semantic decision to a specific stimulus, reflecting its known role in semantic processing (for reviews see Badre and Wagner 2007; Bookheimer 2002).

Correlational analysis demonstrated robust correlations between BOLD activity in the L pIFG seed region and BOLD activity in adjacent regions of the left inferior frontal gyrus (BA 44, 45, and 47), regions within the homologous gyrus of the right hemisphere (BA 44, 45, and 47), bilateral regions of the cingulate gyrus (BA 32), superior frontal gyrus (BA 6), frontal operculum/anterior-insular cortex, lateral and medial banks of the intraparietal sulcus (BA 40), and, notably, bilateral regions of the posterior extent of the middle temporal gyrus (BA 21/37; $P < 0.001$, Fig. 6).

For comparison, the middle occipital gyrus (MOG) of the right hemisphere was interrogated using rs-fcMRI analysis. Although this region was not a focus of "task-evoked" func-

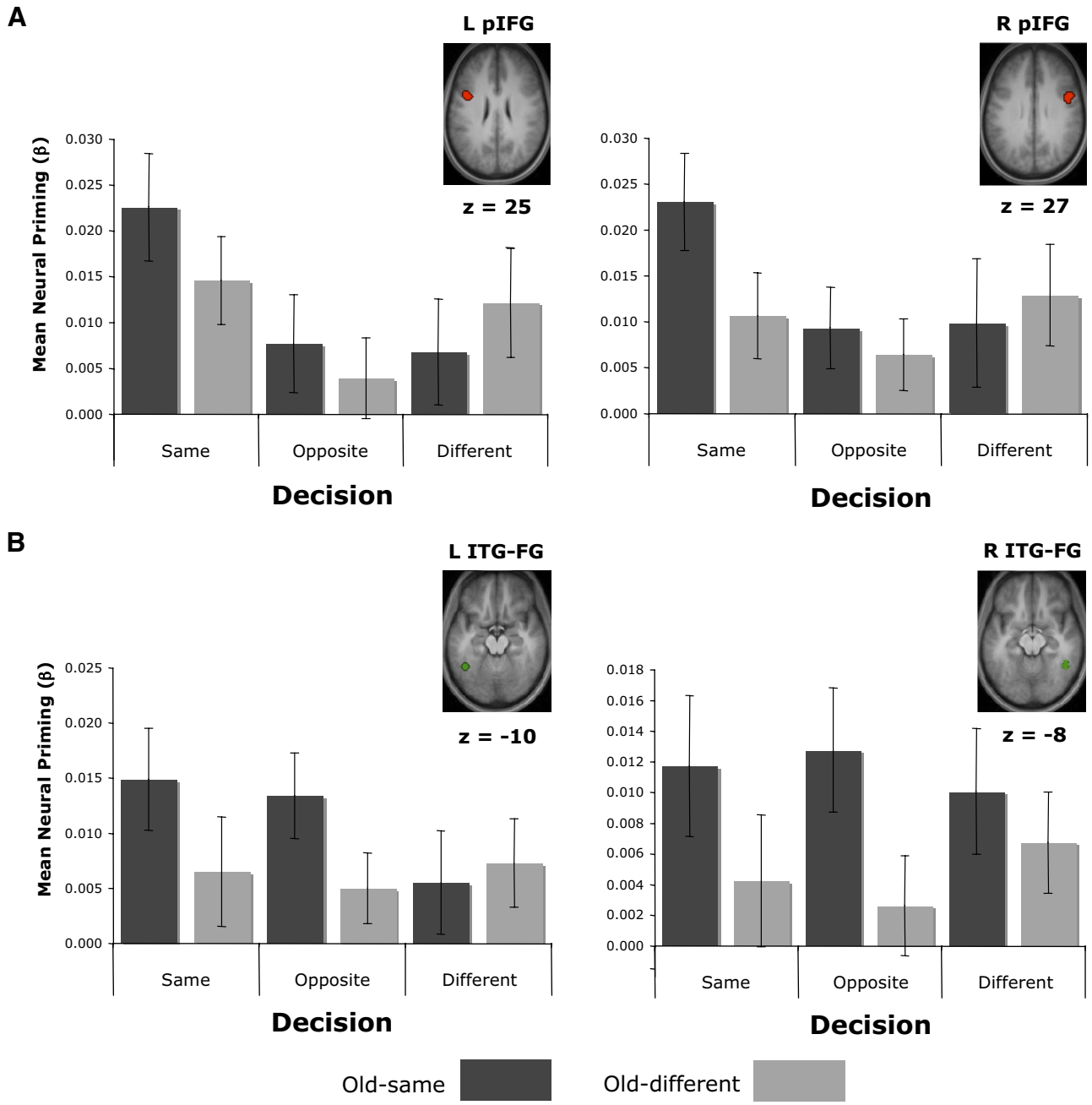

FIG. 4. Posterior inferior-frontal (pIFG; BA 44) and inferior-temporal/fusiform (ITG-FG; BA 21/37) regions demonstrate dissociable patterns of neural priming as a function of decision and stimulus manipulations during the test period. ROIs depicted in red (left and right pIFG) and green (left and right ITG-FG) overlaid on top of average anatomical images. Bar graphs display mean neural priming, calculated as a difference in mean parameter estimates between new and old objects for each decision-type (same-decision, opposite-decision, different-decision) and stimulus-type (old-same and old-different). *A*: neural priming in bilateral pIFG was sensitive to both decision and stimulus manipulations, demonstrating the greatest neural priming during the same-decision performed on old-same objects. *B*: neural priming in bilateral ITG-FG was sensitive only to the stimulus manipulation, demonstrating greater neural priming for old-same than for old-different objects, and was insensitive to changes in the decision type. Error bars correspond to the SE.

tional data set, its selection was motivated as a proof of principle based on its known functional and anatomical properties (Felleman and Van Essen 1991; Mishkin et al. 1983). Accordingly, seeding of this highly perceptual region allowed for a strong contrast to the frontal seed ROI that was correlated with what appeared to be a conceptual system.

ROI selection was based off the nonbiased neural priming map (Fig. 2). Importantly, consistent with its known role in perceptual processing, and similar to bilateral regions of the ITG-FG, examining task-evoked activity in this ROI revealed that neural priming in R MOG demonstrated a significant main effect of stimulus type [$F(1,26) = 4.15$, $P = 0.05$] and no main effect of decision [$F(2,52) = 1.71$, $P > 0.19$] or interaction between the two [$F(2,52) = 1.98$, $P > 0.14$]. Follow-up analysis demonstrated that neural priming in this region was greater during classification of old-same relative to old-different objects [new minus old-same > new minus old-different: $t(80) = 2.11$, $P < 0.05$].

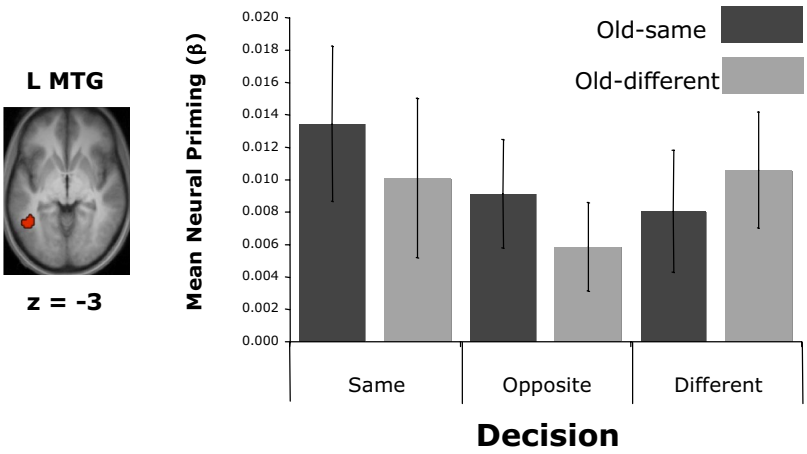

FIG. 5. Neural priming in the left middle temporal gyrus (L MTG; BA 21) is invariant to manipulations of decision or stimulus type. ROI depicted in red overlaid on top of average anatomical image. Neural priming in L MTG was insensitive to manipulations of decision or stimulus type. Notably, neural priming was observed across all trial types. Bar graphs display mean neural priming, calculated as a difference in mean parameter estimates between new and old objects for each decision type (same-decision, opposite-decision, different-decision) and stimulus type (old-same and old-different). Error bars correspond to the SE.

rs-fcMRI analysis revealed that BOLD activity within the R MOG was significantly correlated with regions typically linked to processing along more perceptual dimensions: bilateral regions of the inferior, middle, and superior occipital gyri (BA 18, 19), cuneus (BA 18), precuneus/superior parietal gyrus (BA 7), lingual gyrus (BA 18), fusiform gyrus (BA 19/37), and posterior extent of the inferior- (BA 37) and middle-temporal gyri (BA 21/37) ($P < 0.001$; Fig. 6).

Focusing more closely on the posterior extent of the left lateral temporal lobe revealed that voxels correlating with the L pIFG ROI encapsulated the peak of the previously defined L MTG ROI, yet were distinct from the peak of the ROI localized to the L ITG-FG. In contrast, rs-fcMRI analysis of the MOG ROI revealed significant correlations along the ITG and FG, yet not so in the MTG (Fig. 7).

The task-related functional dissociation between the proximal ROIs of the left temporal cortex, along with the differential correlations with frontal and MOG regions, provide evidence for independent types of processing. The left MTG ROI showed a pattern of activity suggesting its involvement in decision- and stimulus-invariant conceptual processing, whereas activity in the adjacent left ITG-FG ROI indexed the perceptual history of items. Although these regions are located in relatively proximal locations to one another, as a further test of the

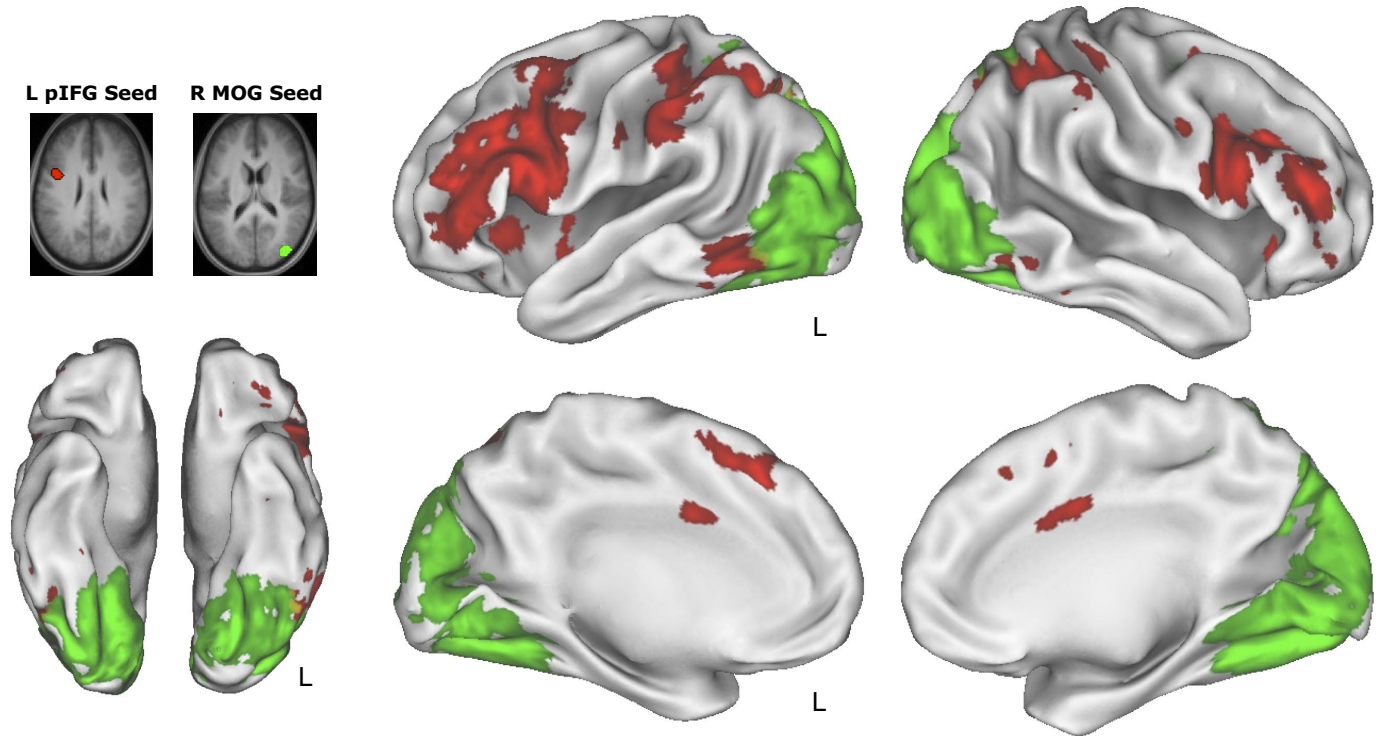

FIG. 6. Distinct cortical systems are correlated with frontal- and occipital-seed regions during rest. Whole brain group statistical image depicts 2 independent resting-state functional connectivity MRI (rs-fcMRI) correlation analyses using seed regions in the left posterior inferior frontal gyrus (L pIFG, BA 44; in red) and right middle occipital gyrus (R MOG, BA 19; in green). Random-effects maps ($P < 0.001$, uncorrected) were obtained after within-subject transformation using Fisher's *r*-to-z, submitted for a second-level analysis, and then overlaid on partially inflated cortical renderings of the left and right hemispheres. Distinct patterns of correlated activity were observed: Among other regions, L pIFG was correlated with bilateral regions of the inferior-frontal gyrus, middle-temporal gyrus, and medial and lateral banks of the intraparietal sulcus. By contrast, R MOG was correlated with bilateral regions of the occipital cortex, and lingual, fusiform, and inferior-temporal gyri. pIFG correlations are depicted in red, MOG correlations are depicted in green, overlap of the 2 correlation analyses are depicted in yellow. *Top*: lateral views of the left and right hemispheres. *Bottom*: ventral and medial views of the left and right hemispheres.

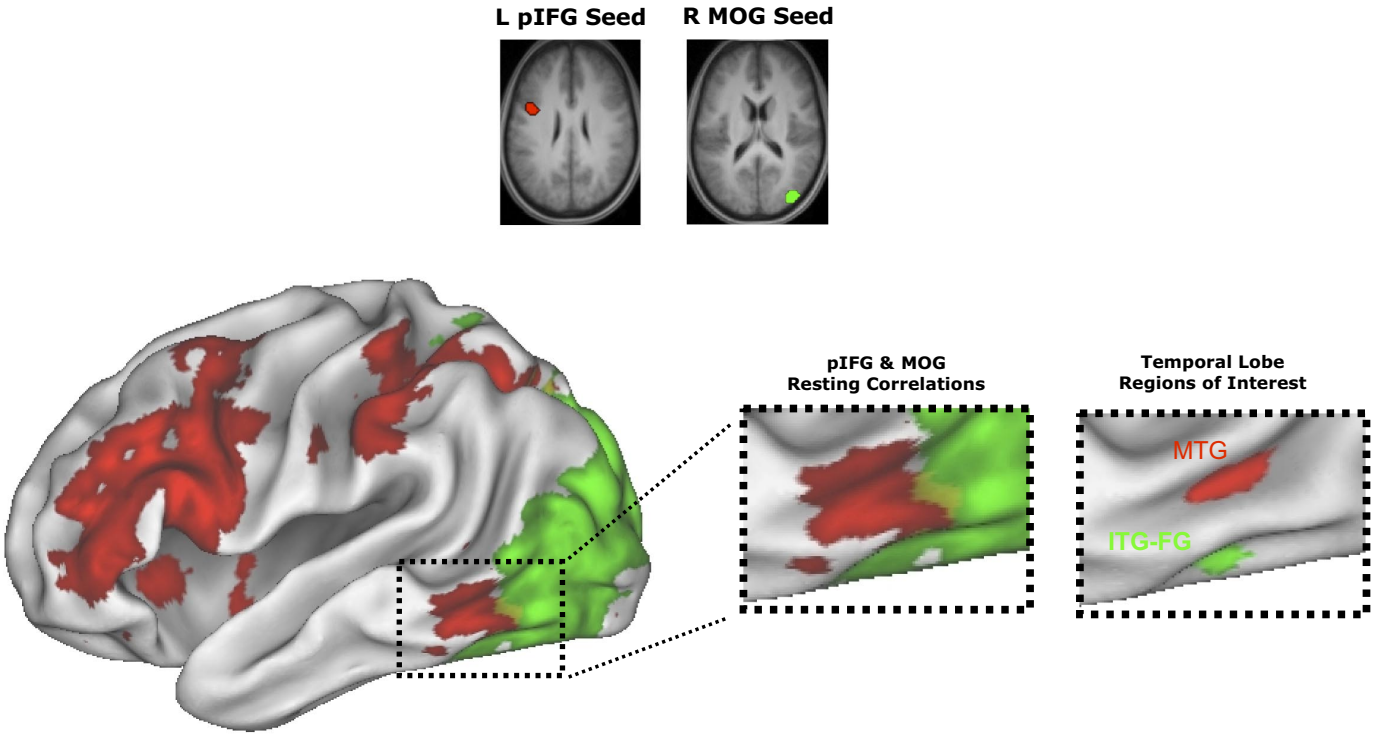

FIG. 7. Frontal and occipital resting period correlation patterns overlap with middle-temporal (MTG) and inferior-temporal/fusiform (ITG-FG) regions of interest, respectively. rs-fcMRI correlation maps were created using frontal and occipital seed regions (see Fig. 6 for details). Focusing on the posterior extent of the left lateral temporal cortex (*left inset*) revealed that frontal correlations overlapped with the L MTG ROI that demonstrated decision- and stimulus-invariant neural priming during the test period (*right inset*, in red), whereas occipital correlations overlapped with the L ITG-FG ROI that demonstrated stimulus-sensitive neural priming during the test period (*right inset*, in green).

distinct systems hypothesis, two independent rs-fcMRI analyses were conducted by seeding each region to observe its pattern of functional correlations with the rest of the brain. This analysis, then, served not only as a form of replication of the initial rs-fcMRI analysis using distinct and independent seed regions that appear to be linked to the previously uncovered systems, but was also motivated by the hypothesis that the neural-priming invariance observed in the L MTG ROI may be related to more semantic or conceptual processing, such that it would be correlated more closely with activity in frontal but not visual regions. In contrast, given the sensitivity of L ITG-FG to changes in the stimulus format (i.e., perceptual features) independent of overlap in the abstract representation, we expected this region to correlate with visual regions.

Similar to the rs-fcMRI pattern observed when seeding left pIFG, in addition to correlating with its homologous region in the right hemisphere, the left MTG demonstrated correlations with regions including those that have been linked to semantic/conceptual but not perceptual processing: bilateral regions of the inferior frontal gyrus, middle temporal gyrus, and the medial and lateral banks of the intraparietal sulcus ($P < 0.001$). In contrast, the ROI situated within the left ITG-FG predominantly correlated with regions linked to perceptual processing. Correlations were observed between this seed region and bilateral regions of the occipital, lingual, fusiform, and inferior temporal gyrus, and a caudal portion of the left pIFG ($P < 0.001$, Fig. 8).

RESTING-STATE FUNCTIONAL CONNECTIVITY REPLICATION ANALYSIS. To demonstrate that the patterns of resting-state correlations were indicative of distinct systems and not a product of thresholding, a formal replication analysis was conducted using an independent data set. Two separate correlation maps were computed using seeds placed in the L MTG and L ITG-FG. Target ROIs, located in the L IFG and R MOG, were obtained from the original data set (Fig. 9*A*). Mean z-transformed correlations [z(r)] were extracted from each target ROI and submitted to a two-way ANOVA including factors of seed (L MTG and L ITG-FG) and target (L IFG and R MOG). Analyses revealed a main effect of seed [$F(1,23) = 12.45$, $P = 0.002$], no main effect of target [$F(1,23) = 1.29$, $P = 0.27$], and a significant seed $\times$ target interaction [$F(1,23) = 28.82$, $P < 0.001$]. Planned comparisons revealed that the correlation between L MTG and L IFG was significantly greater than that of L ITG-FG and L IFG [$t(23) = 7.92$, $P < 0.001$], whereas the correlation between L ITG-FG and R MOG was significantly greater than that of L MTG and R MOG [$t(23) = 2.09$, $P = 0.05$; Fig. 9*B*]. This independent test confirmed that regions within the conceptual (L IFG and L MTG) and perceptual (R MOG and L ITG-FG) systems exhibited greater strengths of resting-state correlations within than between one another.

DISCUSSION

A single experience can have multiple influences on behavior. Here we used a combination of behavioral and imaging approaches to identify distinct brain systems that are simultaneously influenced by the same experience. Manipulations of decision and stimulus types were used to identify regions sensitive to changes in conceptual and perceptual processes,

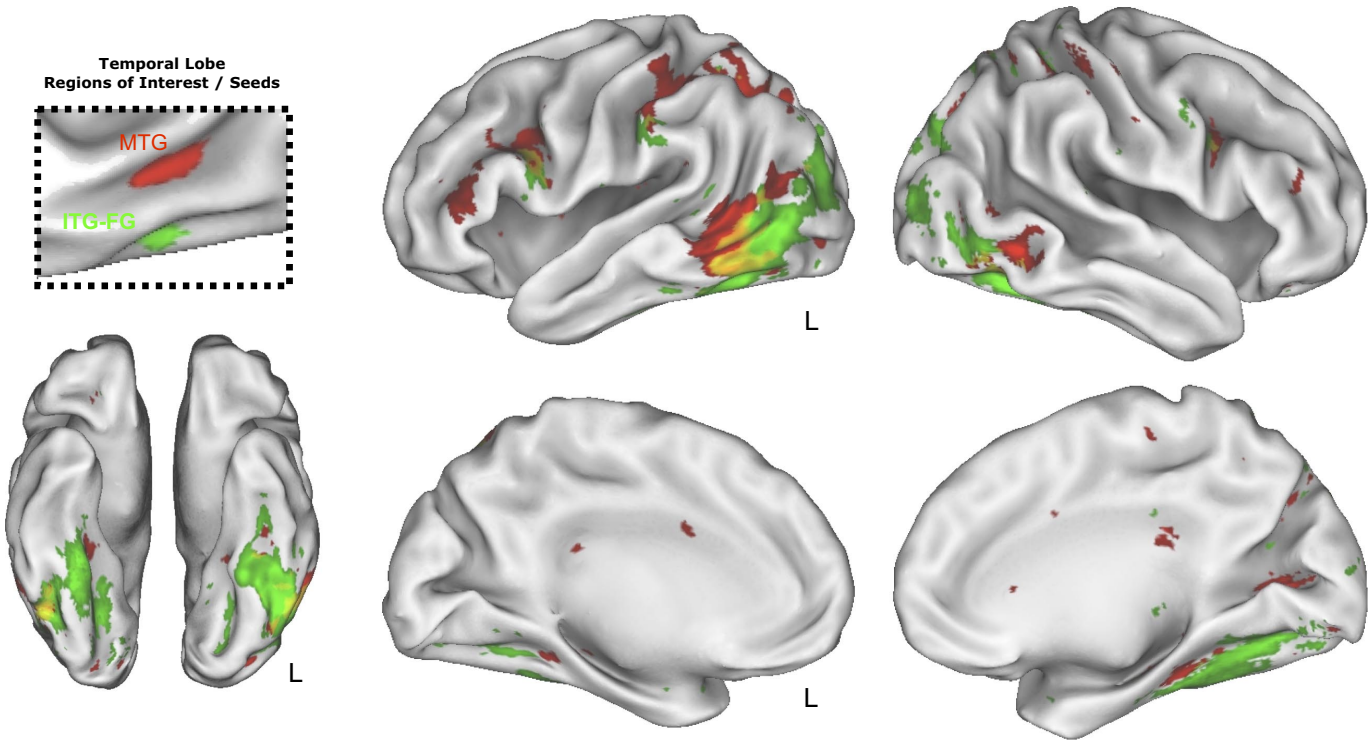

FIG. 8. Distinct cortical systems are correlated with middle-temporal gyrus and inferior-temporal/fusiform gyrus during rest. Whole brain group statistical image depicts 2 independent rs-fcMRI correlation analyses using seed regions in the left middle temporal gyrus (L MTG, BA 21; in red) and left inferior-temporal/fusiform gyrus (L ITG-FG, BA 21/37; in green). Random-effects maps ($P < 0.001$, uncorrected) were obtained after within-subject transformation using Fisher's *r*-to-z, submitted for a second-level analysis, and then overlaid on partially inflated cortical renderings of the left and right hemispheres. Mirroring the rs-fcMRI correlation patterns observed in L pIFG and R MOG, respectively, distinct patterns of correlated activity were observed: Among other regions, L MTG was correlated with bilateral regions of the inferior-frontal gyrus, middle-temporal gyrus, and medial and lateral banks of the intraparietal sulcus. By contrast, L ITG-FG was correlated with bilateral regions of the occipital cortex, and lingual, fusiform, and inferior-temporal gyri. MTG correlations are depicted in red, ITG-FG correlations are depicted in green, overlap of the 2 correlation analyses are depicted in yellow. *Top*: lateral views of the left and right hemispheres. *Bottom*: ventral and medial views of the left and right hemispheres.

respectively. Bilateral regions of posterior inferior frontal gyrus (pIFG) were sensitive to the exact mapping of the decision to the stimulus, whereas bilateral regions in inferior-temporal gyrus and fusiform gyrus (ITG-FG) were found to demonstrate sensitivity to changes in the stimulus independent of the decision made. Resting-state functional connectivity (rs-fcMRI) analysis was then used to determine whether the regions demonstrating dissociated forms of priming are components of distinct brain systems. Consistent with this hypothesis, the regions showing differential modulation due to decision and stimulus manipulations were embedded within two distinct brain systems that likely subserve their respective priming effects. We elaborate on the implications of these results in the following text.

Dissociating conceptual and perceptual components of neural priming

Neural priming in bilateral regions of the inferior frontal gyrus (IFG) was modulated by changes in the semantic decision that were made about objects. Extensive research in humans has linked the IFG to executive processes guiding semantic and phonological processing (Badre and Wagner 2007; Bookheimer 2002; Demb et al. 1995; Petersen et al. 1988; Raichle et al. 1994). These processes include controlled retrieval of semantic (BA 47; Demb et al. 1995; Devlin et al. 2003; Poldrack et al. 1999; Wagner et al. 2001) and phonological (Gold et al. 2002) information, selection from competing alternatives (BA 45; Badre et al. 2005; Thompson-Schill et al. 1998), and the representation of phonetic (Left BA 44; Devlin et al. 2003; Gough et al. 2005; Kelley et al. 1998; Poldrack et al. 1999; Wig et al. 2004) and iconic (Right BA 44; Kelley et al. 1998; Wig et al. 2004) stimulus properties.

It has been suggested that neural priming in the IFG mediates the increased fluency in stimulus-specific semantic or lexical operations that are engendered by repeated classification (Buckner et al. 1998a; van Turennout et al. 2000; Wagner et al. 2000; Wig et al. 2005). Although IFG neural priming may reflect tuning of the semantic representation, retrieval of it, or a combination of these two, recent evidence suggests that priming in the posterior extent of the IFG (pIFG; BA 44) is sensitive to changes in stimulus-to-response learning (Dobbins et al. 2004; Horner and Henson 2008), consistent with facilitation that operates at the stage of the impending decision.

In the present study, neural priming in bilateral regions of the pIFG demonstrated an interaction between decision and stimulus types. Similar to its effects on behavioral priming, classification during the opposite- and different-decision conditions mitigated the magnitude of neural priming in pIFG. In parallel, the stimulus manipulation also influenced pIFG neural priming, although this effect was limited to the same-decision condition wherein classification of old-different objects (same-name exemplars as the studied objects) resulted in less neural priming in the pIFG than old-same

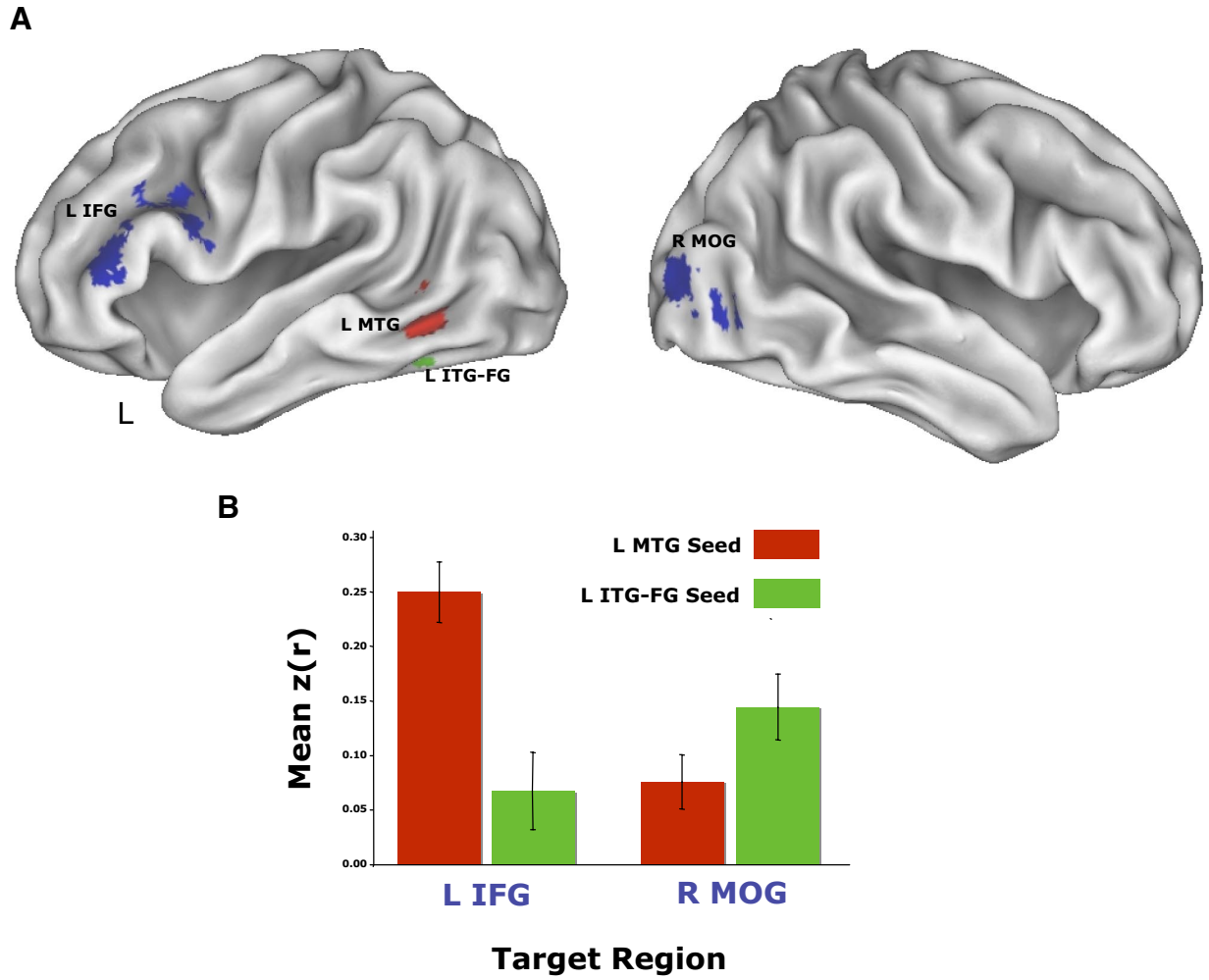

FIG. 9. Distinct cortical regions are correlated with middle-temporal gyrus and inferior-temporal/fusiform gyrus during rest: replication analysis using an independent data set. A replication analysis of temporal cortex rs-fcMRI patterns was conducted using independent data sets. *A*: ROI definition began by initially generating 2 separate maps using seeds placed in the L MTG (in red) and L ITG-FG (in green) to obtain target regions of interest in the left inferior frontal gyrus (L IFG; in blue) and right middle occipital gyrus (R MOG; in blue). ROI definition was conducted on the original data set ($n = 20$; Fig. 8). *B*: resting-state correlation patterns were tested for replication in a separate, independent group of participants ($n = 24$). Replication analysis entailed generating 2 separate maps using seeds placed in the L MTG and L ITG-FG, and then probing the strength of correlations between each of these seeds and the target L IFG and R MOG ROIs defined from the original data set. The L IFG was found to exhibit significantly greater resting-state correlations with the L MTG seed relative to the L ITG-FG seed. In contrast, R MOG exhibited significant greater resting-state correlations with the L ITG-FG seed relative to the L MTG seed. Error bars correspond to the SE.

objects. Accordingly, these results suggest that prefrontal contributions to priming and the behavioral facilitation that repetition affords at least partly relate to mapping of a specific decision onto a specific stimulus. This observation helps to augment the account of pIFG processing, providing support for stimulus-to-decision sensitivity that is "hyper-specific" (Glisky et al. 1986) for identical objects. With extended repetition, neural priming in pIFG likely reflects a direct link between repetition of a given object and the associated decision, potentially bypassing other processing stages that typically accompany repetition.

It is possible that prefrontal contributions to priming might also reflect sensitivity to repeating the same response (e.g., see Supplemental Results) such that distinct regions of prefrontal cortex support decision- versus response specificity independently. Although the present design prevented us from exploring the effect of response changes across repetitions due to the insufficient number of trial types across bins that would have emerged to estimate the BOLD data, a recent report provides support for this idea. By crossing changes in decision and response, Race and colleagues (2008) noted a dissociation within frontal cortices whereby regions of L pIFG (BA 44 and 45) demonstrated sensitivity to decision changes as was reported here, whereas regions of the premotor cortex and anterior-cingulate were sensitive to changes of the specific response (yes/no). Interestingly, these authors also reported decision- and response-invariant priming within a more anterior portion of the left inferior frontal gyrus (L BA 47), providing evidence for a role for this region in more generalized retrieval operations.

In contrast to prefrontal cortices, bilateral regions of the ITG-FG demonstrated sensitivity to stimulus, but not decision, manipulations. Substantial neuroscientific research has linked this set of regions to the identification and recognition of visual objects (for reviews see Grill-Spector and Malach 2004; Mishkin et al. 1983). Although defining the precise nature of cortical representations for visual stimuli has been a topic of consid-

erable debate (Haxby et al. 2001; Kanwisher et al. 1997; Malach et al. 2002; Tarr and Gauthier 2000), experimental paradigms using repetition suppression (adaptation or neural-priming) as a marker for the stored representations have begun to reveal an organized topography within the ventral stream. Transformations along dimensions of luminance (Grill-Spector et al. 1999), size (Grill-Spector et al. 1999; Vuilleumier et al. 2002), shape (Kourtzi and Kanwisher 2001), position (Grill-Spector et al. 1999), and viewpoint (Epstein et al. 2003; Grill-Spector et al. 1999; Vuilleumier et al. 2002) have revealed different degrees of cortical invariance for perceptual manipulations following repetition in humans using BOLD fMRI. These results have meshed well with single-cell recording of macaque inferotemporal (IT) cortex. Neuronal repetition suppression has been shown to accompany presentation of visual objects (Baylis and Rolls 1987; Li et al. 1993; Miller et al. 1991) and neurons in IT cortex exhibit translation and size invariance (Desimone et al. 1984; Gross et al. 1972; Ito et al. 1995; Lueschow et al. 1994).

Along these lines, exemplar manipulations, whereby repeated objects are same-name exemplars of objects initially viewed, have provided evidence that neural priming effects within ventral temporal and occipital cortices likely engage a presemantic level of representation (Schacter 1992; Tulving and Schacter 1990) and are sensitive to repetition of specific object identity (Koutstaal et al. 2001; Simons et al. 2003; Vuilleumier et al. 2002). In the present experiment, the stimulus transformation was of this latter type: repeated objects were either the same objects as those viewed at study or different-exemplars of the previously viewed objects. Although both old-same and old-different object types share an abstract level of representation (i.e., both are same-name exemplars of a given object), old-same objects demonstrated greater neural priming in ITG-FG ROIs relative to old-different objects. Further, neural priming in these regions was independent of the decision made with respect to the object. Together, these results demonstrate ITG-FG sensitivity to repetition of aspects of perceptual but not conceptual attributes of the target items. Specifically, this region demonstrated sensitivity to study–test overlap of the physical identity a given object.

It is worth noting that a number of studies have reported a left–right hemispheric gradient of neural-priming invariance across a variety of manipulations (Koutstaal et al. 2001; Simons et al. 2003; Vuilleumier et al. 2002; for review see Schacter et al. 2007). The ITG-FG ROIs probed in the present report did not exhibit this pattern because they failed to exhibit a hemisphere $\times$ stimulus interaction. The source of this discrepancy is likely related to both the nature of the stimulus manipulation and an anterior–posterior distinction within the ventral temporal cortices. Selection of ROIs was motivated by previous reports using exemplar manipulations (see Table 1). Critically, peaks were selected to isolate those regions that would likely mediate presemantic perceptual priming effects (based on reported coordinates of those regions demonstrating greater activity for old-different objects; same-name exemplars of previously studies objects vs. old-same objects). These ITG-FG peaks were along the posterior and dorsal extent of the inferior temporal cortex/fusiform gyrus.

Consistent with the present report, Vuilleumier and colleagues (2002) reported no exemplar priming in homologous posterior fusiform regions that were proximal to the ITG-FG ROIs interrogated here, and a study probing ROIs extending even more posterior and medially along the fusiform gyrus and into occipital cortices (a region dubbed "the lateral occipital complex") also did not report significant neural priming for exemplar objects (Grill-Spector et al. 1999). A more anterior segment of the fusiform gyrus appears to be sensitive to object properties that are more conceptual or semantic in nature, demonstrating priming across exemplars of a given object, as well as exhibiting a left–right hemispheric asymmetry in the magnitude of this priming (i.e., greater neural priming for same-name exemplar objects in the left than in the right; e.g., see Simons et al. 2003; Fig. 4). Interestingly, a left–right gradient of neural priming has been reported in more posterior fusiform subdivisions as well (Vuilleumier et al. 2002), although the object transformations have been tailored toward more perceptual (changing the viewpoint of an object) than conceptual (i.e., changing the identity of a repeated object as is done with the exemplar manipulation) properties. Together, these results suggest that a left-to-right gradient of invariance may exist, although it abides by the rules of a hierarchical organization of stimulus representations (Felleman and Van Essen 1991; Ungerleider 1995), where areas along the object processing stream differ in their degree of sensitivity to object transformation (see Schacter et al. 2007).

The L ITG-FG ROI reported here is in close proximity to temporal cortex regions highlighted by two recent studies exploring neural priming and response learning (Horner and Henson 2008; Race et al. 2008). The results of the present report converge with these others in demonstrating that this region failed to show sensitivity to decision or response changes. Notably, Dobbins and colleagues (2004) reported decision sensitivity within a more medial region of the left fusiform gyrus. Exploratory analysis failed to uncover a comparable pattern in a proximal region within the present data set; as such, it still remains unclear whether distinct regions of the ventral cortices exhibit sensitivity to patterns of stimulus repetition *and* response learning, or whether subtle differences in experimental paradigm (e.g., number of repetitions) can have an influence on neural priming measures.

In contrast to the profile of neural priming within pIFG and ITG-FG, neural priming in L MTG was observed across all trial types and was invariant to manipulations of either the decision type or the stimulus type. It is tempting to speculate that L-MTG retains an abstract semantic representation (Gold et al. 2006; Martin 2007), such that neural priming reflects amodal (Badgaiyan et al. 2001; Buckner et al. 2000), postperceptual tuning across exemplars within a given category (Wheatley et al. 2005), and is unaffected by changes in the decision (Thompson-Schill et al. 1999). Although caution is warranted regarding interpretation of pattern of activity observed in L MTG given the nature of its ROI selection (see METHODS and RESULTS), when L MTG was defined using the pattern of L pIFG resting correlations (Fig. 6), a similar pattern emerged (see Supplemental Results), strengthening the evidence for that L MTG exhibits generalized neural priming across stimulus and decision manipulations (also see Race et al. 2008; Thompson-Schill et al. 1999). Notably, the present report departs from these others in demonstrating that the priming invariance extends across changes across particular exemplars that share similar semantic representations.

Frontal and temporal regions are embedded within distinct large-scale systems

Frontal and temporal regions of interest that demonstrated dissociable profiles of task-evoked activity based on decision and stimulus manipulations were probed using rs-fcMRI analysis. Analysis of resting-state correlation patterns revealed that the regions of interest were embedded within two distinct functional systems: one that included bilateral regions of the inferior frontal gyrus, middle temporal lobe, and lateral parietal cortex, whereas the other included bilateral regions of the occipital lobe, inferior temporal lobe, and lingual and fusiform gyri.

The correlations between inferior temporal lobe and posterior visual cortices are consistent with the known functional-anatomical architecture of the visual system (Felleman and Van Essen 1991; Ungerleider 1995) and likely reflect a marker of the ventral visual stream's coordinated activity in mediating visual perception. Consistent with this, both rs-fcMRI seed regions that demonstrated sensitivity to the stimulus manipulation independent of decision type (inferior temporal gyrus and middle occipital gyrus) demonstrated comparable patterns of resting-state correlations.

We focus our discussion of rs-fcMRI on the frontal and middle-temporal correlations. Prior research exploring conceptual processing has demonstrated the contributions of the inferior frontal gyrus and middle temporal gyrus toward semantic operations (Martin 2007; Petersen et al. 1988; Wagner et al. 2001), whereas postmortem anatomical dissection (Dejerine 1895), intraoperative electrostimulation of subcortical (white-matter) connectivity (Duffau 2008), and diffusion tensor imaging (Glasser and Rilling 2008) have highlighted the prominent white-matter fiber bundle that connects inferior frontal and lateral posterior temporal regions in humans (i.e., the arcuate fasciculus). Consistent with this observation, damage to frontal or temporal nodes, or the pathway connecting them, results in dissociable forms of language impairment (Geschwind 1970). The rs-fcMRI patterns reported here augment this research: independent analyses seeding frontal and middle-temporal regions revealed strong correlations with one another. Together with a recent study that reported changes in frontal–temporal synchrony across repetitions (Ghuman et al. 2008) and the demonstration that behavioral priming and neural priming in both frontal and middle-temporal regions is ablated following transcranial magnetic stimulation to frontal regions (Wig et al. 2005), these results provide support for the idea that conceptual priming may relate to changes in the coupling between frontal and temporal regions.

What are the types of operations that may be supported by prefrontal regions during semantic classification? The network correlating with prefrontal regions is particularly intriguing with respect to this question in light of the accumulating evidence that repetition can influence processes associated with decision stages. Resting-state correlations revealed that conceptual repetition effects arose within regions of a "frontoparietal control" system (e.g., Damoiseaux et al. 2006; Dosenbach et al. 2007; Vincent et al. 2008) that participates in decision operations. This system is active during tasks that require processing multiple independent contingencies (Kroger et al. 2002) or conflicting stimulus–response mappings (Crone et al. 2006). Here in the context of a semantic classification task that required participants to make decisions about novel categories, repetition was shown to attenuate activity within regions of the frontoparietal control system, providing further support that conceptual priming reflects facilitation in decision processes.

In summary, the results of the present study demonstrate how a single experience can simultaneously modify multiple operations and give rise to dissociated brain changes. Repetition priming as explored in the behavioral literature likely reflects the operation and interactions among these multiple neural components. Here, we highlight and provide strong evidence for at least two of these components. Furthermore, we demonstrate that these components are embedded within dissociable systems that mediate distinct types of processing.

ACKNOWLEDGMENTS

We thank D. Stevens and I. Kahn for assistance with data collection, members of the Cognitive Neuroscience Laboratory and Memory Laboratory at the Department of Psychology in Harvard University for valuable discussion, and two anonymous reviewers for thoughtful comments on an earlier version of this manuscript.

GRANTS

This work was supported by an Institute for Aging Postdoctoral Fellowship from the Canadian Institute for Health Research to G. S. Wig, the Howard Hughes Medical Institute, and a National Institute of Mental Health Grant MH-060941 to D. L. Schacter.

REFERENCES

Badgaiyan RD, Schacter DL, Alpert NM. Priming within and across modalities: exploring the nature of rCBF increases and decreases. *NeuroImage* 13: 272–282, 2001.

Badre D, Poldrack RA, Paré-Blagoev EJ, Insler RZ, Wagner AD. Dissociable controlled retrieval and generalized selection mechanisms in ventrolateral prefrontal cortex. *Neuron* 47: 907–918, 2005.

Badre D, Wagner AD. Left ventrolateral prefrontal cortex and the cognitive control of memory. *Neuropsychologia* 45: 2883–2901, 2007.

Baylis GC, Rolls ET. Responses of neurons in the inferior temporal cortex in short term and serial recognition memory tasks. *Exp Brain Res* 65: 614–622, 1987.

Blaxton TA. Investigating dissociations among memory measures: support for a transfer appropriate processing framework. *J Exp Psychol Learn Mem Cogn* 15: 657–668, 1989.

Bookheimer S. Functional MRI of language: new approaches to understanding the cortical organization of semantic processing. *Annu Rev Neurosci* 25: 151–188, 2002.

Brainard DH. The Psychophysics Toolbox. *Spat Vis* 10: 433–436, 1997.

Buckner RL, Goodman J, Burock M, Rotte M, Koutstaal W, Schacter D, Rosen B, Dale AM. Functional-anatomic correlates of object priming in humans revealed by rapid presentation event-related fMRI. *Neuron* 20: 285–296, 1998a.

Buckner RL, Koutstaal W, Schacter DL, Dale AM, Rotte M, Rosen BR. Functional-anatomic study of episodic retrieval. II. Selective averaging of event-related fMRI trials to test the retrieval success hypothesis. *NeuroImage* 7: 163–175, 1998b.

Buckner RL, Koutstaal W, Schacter DL, Rosen BR. Functional MRI evidence for a role of frontal and inferior temporal cortex in amodal components of priming. *Brain* 123: 620–640, 2000.

Buckner RL, Petersen SE, Ojemann JG, Miezin FM, Squire LR, Raichle ME. Functional anatomical studies of explicit and implicit memory retrieval tasks. *J Neurosci* 15: 12–29, 1995.

Cave CB, Squire LR. Intact and long-lasting repetition priming in amnesia. *J Exp Psychol Learn Mem Cogn* 18: 509–520, 1992.

Chawla D, Rees G, Friston KJ. The physiological basis of attentional modulation in extrastriate visual areas. *Nat Neurosci* 2: 671–676, 1999.

Crone EA, Wendelken C, Donohue SE, Bunge SA. Neural evidence for dissociable components of task-switching. *Cereb Cortex* 16: 475–486, 2006.

Damoiseaux JS, Rombouts SA, Barkhof F, Scheltens P, Stam CJ, Smith SM, Beckmann CF. Consistent resting-state networks across healthy subjects. *Proc Natl Acad Sci USA* 103: 13848–13853, 2006.

Dejerine J. *Anatomie des Centres Nerveux.* Paris: Rueff et Cie, 1895.

Demb JB, Desmond JE, Wagner AD, Vaidya CJ, Glover GH, Gabrieli JD. Semantic encoding and retrieval in the left inferior prefrontal cortex: a functional MRI study of task difficulty and process specificity. *J Neurosci* 15: 5870–5878, 1995.

Desimone R. Neural mechanisms for visual memory and their role in attention. *Proc Natl Acad Sci USA* 93: 13494–13499, 1996.

Desimone R, Albright TD, Gross CG, Bruce C. Stimulus-selective properties of inferior temporal neurons in the macaque. *J Neurosci* 4: 2051–2062, 1984.

Devlin JT, Matthews PM, Rushworth MF. Semantic processing in the left inferior prefrontal cortex: a combined functional magnetic resonance imaging and transcranial magnetic stimulation study. *J Cogn Neurosci* 15: 71–84, 2003.

Dobbins IG, Schnyer DM, Verfaellie M, Schacter DL. Cortical activity reductions during repetition priming can result from rapid response learning. *Nature* 428: 316–319, 2004.

Donaldson DI, Petersen SE, Ollinger JM, Buckner RL. Dissociating state and item components of recognition memory using fMRI. *NeuroImage* 13: 129–142, 2001.

Dosenbach NU, Fair DA, Miezin FM, Cohen AL, Wenger KK, Dosenbach RA, Fox MD, Snyder AZ, Vincent JL, Raichle ME, Schlaggar BL, Petersen SE. Distinct brain networks for adaptive and stable task control in humans. *Proc Natl Acad Sci USA* 104: 11073–11078, 2007.

Duffau H. The anatomo-functional connectivity of language revisited. New insights provided by electrostimulation and tractography. *Neuropsychologia* 46: 927–934, 2008.

Epstein R, Graham KS, Downing PE. Viewpoint-specific scene representations in human parahippocampal cortex. *Neuron* 37: 865–876, 2003.

Felleman DJ, Van Essen DC. Distributed hierarchical processing in the primate cerebral cortex. *Cereb Cortex* 1: 1–47, 1991.

Fleischman DA, Gabrieli JD. Repetition priming in normal aging and Alzheimer's disease: a review of findings and theories. *Psychol Aging* 13: 88–119, 1998.

Fox MD, Raichle ME. Spontaneous fluctuations in brain activity observed with functional magnetic resonance imaging. *Nat Rev Neurosci* 8: 700–711, 2007.

Fox MD, Snyder AZ, Vincent JL, Corbetta M, Van Essen DC, Raichle ME. The human brain is intrinsically organized into dynamic, anticorrelated functional networks. *Proc Natl Acad Sci USA* 102: 9673–9678, 2005.

Friston KJ, Holmes AP, Worsley KJ, Poline J-P, Frith C, Frackowiak RSJ. Statistical parametric maps in functional imaging: a general linear approach. *Hum Brain Mapp* 2: 189–210, 1995.

Gabrieli JDE, Fleischman DA, Keane MM, Reminger SL, Morrell F. Double dissociation between memory systems underlying explicit and implicit memory in the human brain. *Psychol Sci* 6: 76–82, 1995.

Geschwind N. The organization of language and the brain. *Science* 170: 940–944, 1970.

Ghuman AS, Bar M, Dobbins IG, Schnyer DM. The effects of priming on frontal-temporal communication. *Proc Natl Acad Sci USA* 105: 8405–8409, 2008.

Glasser MF, Rilling JK. DTI tractography of the human brain's language pathways. *Cereb Cortex* 18: 2471–2482, 2008.

Glisky EL, Schacter DL, Tulving E. Computer learning by memory-impaired patients: acquisition and retention of complex knowledge. *Neuropsychologia* 24: 313–328, 1986.

Gold BT, Balota DA, Jones SJ, Powell DK, Smith CD, Andersen AH. Dissociation of automatic and strategic lexical-semantics: functional magnetic resonance imaging evidence for differing roles of multiple frontotemporal regions. *J Neurosci* 26: 6523–6532, 2006.

Gough PM, Nobre AC, Devlin JT. Dissociating linguistic processes in the left inferior frontal cortex with transcranial magnetic stimulation. *J Neurosci* 25: 8010–8016, 2005.

Graf P, Schacter DL. Implicit and explicit memory for new associations in normal and amnesic subjects. *J Exp Psychol Learn Mem Cogn* 11: 501–518, 1985.

Grill-Spector K, Henson R, Martin A. Repetition and the brain: neural models of stimulus-specific effects. *Trends Cogn Sci* 10: 14–23, 2006.

Grill-Spector K, Kushnir T, Edelman S, Avidan G, Itzchak Y, Malach R. Differential processing of objects under various viewing conditions in the human lateral occipital complex. *Neuron* 24: 187–203, 1999.

Grill-Spector K, Malach R. The human visual cortex. *Annu Rev Neurosci* 27: 649–677, 2004.

Gross CG, Rocha-Miranda CE, Bender DB. Visual properties of neurons in inferotemporal cortex of the macaque. *J Neurophysiol* 35: 96–111, 1972.

Haxby JV, Gobbini MI, Furey ML, Ishai A, Schouten JL, Pietrini P. Distributed and overlapping representations of faces and objects in ventral temporal cortex. *Science* 293: 2425–2430, 2001.

Henson R, Shallice T, Dolan R. Neuroimaging evidence for dissociable forms of repetition priming. *Science* 287: 1269–1272, 2000.

Henson RN. Neuroimaging studies of priming. *Prog Neurobiol* 70: 53–81, 2003.

Horner AJ, Henson RN. Priming, response learning and repetition suppression. *Neuropsychologia* 46: 1979–1991, 2008.

Ito M, Tamura H, Fujita I, Tanaka K. Size and position invariance of neuronal responses in monkey inferotemporal cortex. *J Neurophysiol* 73: 218–226, 1995.

Kanwisher N, McDermott J, Chun MM. The fusiform face area: a module in human extrastriate cortex specialized for face perception. *J Neurosci* 17: 4302–4311, 1997.

Keane MM, Gabrieli JD, Fennema AC, Growdon JH, Corkin S. Evidence for a dissociation between perceptual and conceptual priming in Alzheimer's disease. *Behav Neurosci* 105: 326–342, 1991.

Kelley WM, Miezin FM, McDermott KB, Buckner RL, Raichle ME, Cohen NJ, Ollinger JM, Akbudak E, Conturo TE, Snyder AZ, Petersen SE. Hemispheric specialization in human dorsal frontal cortex and medial temporal lobe for verbal and nonverbal memory encoding. *Neuron* 20: 927–936, 1998.

Konishi S, Donaldson DI, Buckner RL. Transient activation during block transition. *NeuroImage* 13: 364–374, 2001.

Kourtzi Z, Kanwisher N. Representation of perceived object shape by the human lateral occipital complex. *Science* 293: 1506–1509, 2001.

Koutstaal W, Wagner AD, Rotte M, Maril A, Buckner RL, Schacter DL. Perceptual specificity in visual object priming: functional magnetic resonance imaging evidence for a laterality difference in fusiform cortex. *Neuropsychologia* 39: 184–199, 2001.

Kroger JK, Sabb FW, Fales CL, Bookheimer SY, Cohen MS, Holyoak KJ. Recruitment of anterior dorsolateral prefrontal cortex in human reasoning: a parametric study of relational complexity. *Cereb Cortex* 12: 477–485, 2002.

Li L, Miller EK, Desimone R. The representation of stimulus familiarity in anterior inferior temporal cortex. *J Neurophysiol* 69: 1918–1929, 1993.

Logan GD. Repetition priming and automaticity: common underlying mechanisms? *Cogn Psychol* 22: 1–35, 1990.

Lueschow A, Miller EK, Desimone R. Inferior temporal mechanisms for invariant object recognition. *Cereb Cortex* 4: 523–531, 1994.

Lustig C, Buckner RL. Preserved neural correlates of priming in old age and dementia. *Neuron* 42: 865–875, 2004.

Maccotta L, Buckner RL. Evidence for neural effects of repetition that directly correlate with behavioral priming. *J Cogn Neurosci* 16: 1625–1632, 2004.

Malach R, Levy I, Hasson U. The topography of high-order human object areas. *Trends Cogn Sci* 6: 176–184, 2002.

Martin A. The representation of object concepts in the brain. *Annu Rev Psychol* 58: 25–45, 2007.

Miezin FM, Maccotta L, Ollinger JM, Petersen SE, Buckner RL. Characterizing the hemodynamic response: effects of presentation rate, sampling procedure, and the possibility of ordering brain activity based on relative timing. *NeuroImage* 11: 735–759, 2000.

Miller EK, Li L, Desimone R. A neural mechanism for working and recognition memory in inferior temporal cortex. *Science* 254: 1377–1379, 1991.

Mishkin M, Ungerleider LG, Macko KA. Object vision and spatial vision: two cortical pathways. *Trends Neurosci* 6: 414–417, 1983.

Petersen SE, Fox PT, Posner MI, Mintun M, Raichle ME. Positron emission tomographic studies of the cortical anatomy of single-word processing. *Nature* 331: 585–589, 1988.

Poldrack RA, Wagner AD, Prull MW, Desmond JE, Glover GH, Gabrieli JD. Functional specialization for semantic and phonological processing in the left inferior prefrontal cortex. *NeuroImage* 10: 15–35, 1999.

Race EA, Shanker S, Wagner AD. Neural priming in human frontal cortex: multiple forms of learning reduce demands on the prefrontal executive system. *J Cogn Neurosci* (September 29, 2008). doi:10.1162/jocn.2009.21132.

Raichle ME, Fiez JA, Videen TO, MacLeod AM, Pardo JV, Fox PT, Petersen SE. Practice-related changes in human brain functional anatomy during nonmotor learning. *Cereb Cortex* 4: 8–26, 1994.

Roediger HL 3rd. Implicit memory retention without remembering. *Am Psychol* 45: 1043–1056, 1990.

Roediger HL 3rd, Blaxton TA. Retrieval modes produce dissociations in memory. In: *Memory and Cognitive Processes: The Ebbinghaus Centennial Conference*, edited by Gorfein D, Hoffman RR. Hillsdale, NJ: Erlbaum, 1987, p. 349–379.

Roediger HL 3rd, McDermott KB. Implicit memory in normal human subjects. In: *Handbook of Neuropsychology*, edited by Boller F, Grafman J. Amsterdam: Elsevier, 1993, p. 63–131.

Schacter DL. Implicit memory: history and current status. *J Exp Psychol Learn Mem Cogn* 13: 501–518, 1987.

Schacter DL. Understanding implicit memory. A cognitive neuroscience approach. *Am Psychol* 47: 559–569, 1992.

Schacter DL, Alpert NM, Savage CR, Rauch SL, Albert MS. Conscious recollection and the human hippocampal formation: evidence from positron emission tomography. *Proc Natl Acad Sci USA* 93: 321–325, 1996.

Schacter DL, Buckner RL. Priming and the brain. *Neuron* 20: 185–195, 1998.

Schacter DL, Buckner RL, Koutstaal W, Dale AM, Rosen BR. Late onset of anterior prefrontal activity during true and false recognition: an event-related fMRI study. *NeuroImage* 6: 259–269, 1997.

Schacter DL, Dobbins IG, Schnyer DM. Specificity of priming: a cognitive neuroscience perspective. *Nat Rev Neurosci* 5: 853–862, 2004.

Schacter DL, Wig GS, Stevens WD. Reductions in cortical activity during priming. *Curr Opin Neurobiol* 17: 171–176, 2007.

Schnyer DM, Dobbins IG, Nicholls L, Davis S, Verfaellie M, Schacter DL. Item to decision mapping in rapid response learning. *Mem Cogn* 35: 1472–1482, 2007.

Simons JS, Koutstaal W, Prince S, Wagner AD, Schacter DL. Neural mechanisms of visual object priming: evidence for perceptual and semantic distinctions in fusiform cortex. *NeuroImage* 19: 613–626, 2003.

Squire LR, Ojemann JG, Miezin FM, Petersen SE, Videen TO, Raichle ME. Activation of the hippocampus in normal humans: a functional anatomical study of memory. *Proc Natl Acad Sci USA* 89: 1837–1841, 1992.

Tarr MJ, Gauthier I. FFA: a flexible fusiform area for subordinate-level visual processing automatized by expertise. *Nat Neurosci* 3: 764–769, 2000.

Thompson-Schill SL, D'Esposito M, Kan IP. Effects of repetition and competition on activity in left prefrontal cortex during word generation. *Neuron* 23: 513–522, 1999.

Thompson-Schill SL, Swick D, Farah MJ, D'Esposito M, Kan IP, Knight RT. Verb generation in patients with focal frontal lesions: a neuropsychological test of neuroimaging findings. *Proc Natl Acad Sci USA* 95: 15855–15860, 1998.

Tulving E, Schacter DL. Priming and human memory systems. *Science* 247: 301–306, 1990.

Turk-Browne NB, Yi DJ, Chun MM. Linking implicit and explicit memory: common encoding factors and shared representations. *Neuron* 49: 917–927, 2006.

Ungerleider LG. Functional brain imaging studies of cortical mechanisms for memory. *Science* 270: 769–775, 1995.

Van Essen DC. A Population Average Landmark- and Surface-based (PALS) atlas of human cerebral cortex. *Neuroimage* 28: 635–662, 2005.

van Turennout M, Ellmore T, Martin A. Long-lasting cortical plasticity in the object naming system. *Nat Neurosci* 3: 1329–1334, 2000.

Vincent JL, Kahn I, Snyder AZ, Raichle ME, Buckner RL. Evidence for a frontoparietal control system revealed by intrinsic functional connectivity. *J Neurophysiol* 100: 3328–3342, 2008.

Vincent JL, Snyder AZ, Fox MD, Shannon BJ, Andrews JR, Raichle ME, Buckner RL. Coherent spontaneous activity identifies a hippocampal-parietal memory network. *J Neurophysiol* 96: 3517–3531, 2006.

Vuilleumier P, Henson RN, Driver J, Dolan RJ. Multiple levels of visual object constancy revealed by event-related fMRI of repetition priming. *Nat Neurosci* 5: 491–499, 2002.

Wagner AD, Desmond JE, Demb JB, Glover GH, Gabrieli JDE. Semantic repetition priming for verbal and pictorial knowledge: a functional MRI study of left inferior prefrontal cortex. *J Cogn Neurosci* 9: 714–726, 1997.

Wagner AD, Koutstaal W, Maril A, Schacter DL, Buckner RL. Task-specific repetition priming in left inferior prefrontal cortex. *Cereb Cortex* 10: 1176–1184, 2000.

Wagner AD, Paré-Blagoev EJ, Clark J, Poldrack RA. Recovering meaning: left prefrontal cortex guides controlled semantic retrieval. *Neuron* 31: 329–338, 2001.

Warrington EK, Weiskrantz L. The effect of prior learning on subsequent retention in amnesic patients. *Neuropsychologia* 12: 419–428, 1974.

Wheatley T, Weisberg J, Beauchamp MS, Martin A. Automatic priming of semantically related words reduces activity in the fusiform gyrus. *J Cogn Neurosci* 17: 1871–1885, 2005.

Wig GS, Grafton ST, Demos KE, Kelley WM. Reductions in neural activity underlie behavioral components of repetition priming. *Nat Neurosci* 8: 1228–1233, 2005.

Wig GS, Miller MB, Kingstone A, Kelley WM. Separable routes to human memory formation: dissociating task and material contributions in the prefrontal cortex. *J Cogn Neurosci* 16: 139–148, 2004.

Wiggs CL, Martin A. Properties and mechanisms of perceptual priming. *Curr Opin Neurobiol* 8: 227–233, 1998.

Zar JH. *Biostatistical Analysis.* Upper Saddle River, NJ: Prentice Hall, 1996.